RESEARCH DIVISION

91602
new 82-10

LEGAL NOTICE

This report was prepared by Ontario Hydro and, while effort has been made to ensure the accuracy and applicability of the material contained herein, neither Ontario Hydro nor any person acting on its behalf

(a) makes any warranty, express or implied, with respect to the accuracy, completeness or usefulness of the information contained in this report or that the use of any information, method or process disclosed in this report

(b) assumes any liability with respect to the use of, or for any damages resulting from the use of, any information, method or process disclosed in this report.

CONFIDENTIAL COPY

ontario hydro
research division

CORROSION OF COPPER AS A USED NUCLEAR FUEL DISPOSAL CONTAINER MATERIAL: EFFECTS OF SULPHIDE IONS AND γ RADIOLYSIS

Report No 89-211-K

K.W. Lam
Engineer
Corrosion and Tritium
Technology Section
Metallurgical Research
Department

ABSTRACT

The corrosion performance of copper as a container material for the disposal of used nuclear fuel has been reviewed. Long-term corrosion data for copper in a saline groundwater-sodium bentonite slurry has been determined. A rate equation was derived for a diffusion limited corrosion reaction for comparison with the empirical data. The effects of oxygen, salinity, temperature, sulphide ions and γ irradiation on copper's corrosion rate were examined. The corrosion products were identified and their morphology was found to have an effect on copper's corrosion behaviour.

job	file	date	report no.
82-139-40161	827.24	July 24, 1990	89-211-K

91602
new 82-10

91-02126/

ontario hydro
research division

EXECUTIVE SUMMARY

CORROSION OF COPPER AS A USED NUCLEAR FUEL DISPOSAL CONTAINER MATERIAL: EFFECTS OF SULPHIDE IONS AND γ RADIOLYSIS

K.W. Lam
Engineer
Corrosion and Tritium
Technology Section
Metallurgical Research Department

Copper is one of the materials being considered for fabricating containers for the geologic disposal of used nuclear fuel. At present, the Canadian specification for the lifetime of the container is 500 years to 1000 years. In order to evaluate whether a copper container will meet this lifetime requirement, an assessment of copper's corrosion properties was undertaken. The work reported here is phase one of a two phase program aimed at providing information for estimating a corrosion allowance thickness that would satisfy the container's lifetime specification. This report is divided into two parts:

- a preliminary assessment, and
- experimental results on the effects of irradiation and sulphide on copper's corrosion rate in a saline groundwater-bentonite slurry.

The following are some specific findings in this work:

1. A corrosion allowance of 2 mm should be sufficient to meet the lifetime specification of the container in a sulphide free environment at 75°C with an oxygen concentration of < 0.1 mg/L. If the environment is equilibrated with an atmosphere of air, a 5 cm allowance is estimated.
2. The corrosion rate of copper will achieve an apparent steady value in one to two months in a stable environment.
3. Oxidant content has a great influence on the corrosion rate of copper and salinity has no apparent effect.
4. The presence of sulphide ions generally increases copper's corrosion rate.
5. Irradiation has a generally beneficial effect on the corrosion of copper.

job	file	date	report no.
82-139-40161	827.24	July 24, 1990	89-211-K

6. The inner layer of corrosion product on copper's surface is porous. Occasionally, this same product can acquire a dual structure with a compact layer formed on top of the porous layer.

7. The porosity of the corrosion product has a large influence on copper's corrosion rate and the morphology of attack.

TABLE OF CONTENTS

		Page
1.0	BACKGROUND	1
	1.1 Used Nuclear Fuel Disposal Concept	1
	1.2 Container Lifetime	2
	1.3 Container Environment	2
	1.4 Container Material	2
2.0	PROGRAM OBJECTIVE AND APPROACH	3
3.0	PRELIMINARY ASSESSMENT	3
	3.1 Thermodynamics	3
	3.1.1 Cathodic Reactions	3
	3.1.2 Anodic Reactions	4
	3.2 Kinetics	5
	3.2.1 Copper Dissolution	5
	3.2.2 Oxygen Reduction	6
	3.2.3 Diffusion	6
	3.3 Other Rate Controlling Parameters	7
	3.3.1 Salinity	7
	3.3.2 Temperature	8
	3.3.3 Sulphide	8
	3.3.4 Radiolysis	8
	3.4 Localized Corrosion	8
	3.4.1 Pitting	8
	3.4.2 Stress Corrosion Cracking	9
4.0	EXPERIMENTAL	9
	4.1 Test Sample	9
	4.2 Test Environment	10
	4.3 Test Duration	11
	4.4 Analytical Techniques	11
	4.4.1 Polarization Resistance	11
	4.4.2 Potential Measurement	11
	4.4.3 Optical Method	11
	4.4.4 Descaling	11
	4.4.5 Pit Depth Measurement	11

5.0 RESULTS 12

5.1 Corrosion Rate-Time Trend 12
5.2 Corrosion Rate 12

5.2.1 Effects of Oxygen 13
5.2.2 Effects of Temperature 13
5.2.3 Effects of Sulphide 13
5.2.4 Effects of Radiolysis 13

5.3 Corrosion Product 13
5.4 Corrosion Morphology 15
5.5 Pitting Rate 15
5.6 Corrosion Potential 16

6.0 DISCUSSION 16

7.0 CONCLUSIONS 18

8.0 ACKNOWLEDGEMENT 19

REFERENCES 20

APPENDIX 1 - ESTIMATION OF DIFFUSION CONTROLLED COPPER CORROSION RATE. 23

A1-1.0 Fixed Diffusion Layer 23
A1-2.0 Semi-infinite Linear Diffusion 24

APPENDIX 2 - PREPARATION OF WN1 SALINE GROUNDWATER 26

APPENDIX 3 - RADIOLYSIS TEST RIG 27

A3-1.0 Location 27
A3-2.0 Cylinder Container 27
A3-3.0 Autoclave 27
A3-4.0 Instrumentation 28

ontario hydro
research division

To Mr. P.D. Stevens-Guille
Radioactive Materials Management Engineer
Nuclear Materials Management Department
Design and Development - Generation

CORROSION OF COPPER AS A USED NUCLEAR FUEL DISPOSAL CONTAINER MATERIAL: EFFECTS OF SULPHIDE IONS AND γ RADIOLYSIS

1.0 BACKGROUND

1.1 USED NUCLEAR FUEL DISPOSAL CONCEPT

At present, Ontario Hydro stores its used nuclear fuel in water pools at the reactor site. The used fuel is highly radioactive, a result of fission products and actinides produced during reactor operation. The half-lives of some of these radioactive elements, especially the actinides, are very long; for example the half-life of plutonium-239 is 24,360 years. Because of the activity and the longevity of some of the radioactive isotopes, the used fuel requires a very long term isolation from the biological environment.

In Canada, as well as in other countries, the present preferable option for the permanent disposal of high level nuclear waste is geologic emplacement[1,2]. Pluton or hard rock formation of the Canadian Shield, because of its historic stability and abundance, is being considered as a type of geologic formation most viable for the disposal of nuclear waste. The plutonic rock has a low permeability, but groundwater, which is a mass transport medium, can penetrate the formation through fissures. To ensure isolation, the present disposal concept calls for a series of engineered barriers to contain the waste, which include:

- a corrosion resistant container to encase the waste; and
- a low water permeable, compacted clay-sand mixture with a high swelling capacity to embed the container.

In a system conceived for this multi-barrier approach, a disposal vault with boreholes in its floor is constructed in a pluton at 0.5 km to 1.0 km deep. A waste package is deposited in each borehole lined with a compacted clay-sand mixture. At the completion of the system, the vault is backfilled with the clay-sand mixture, sealed and grouted. In this approach, both the geologic and engineered systems are intended as barriers to impede the movement of active materials. To assure that only an insignificant amount of radioactive nuclei could escape from this system, an in-depth program was embarked upon to assess the following:

- the role of each barrier;
- potential materials and disposal sites; and
- the rate of mass transport through each barrier.

This report is concerned with the mass transport aspect, in terms of the corrosion kinetics of copper as a container material.

1.2 CONTAINER LIFETIME

With an intact metallic container, immobilization of radioactive nuclei is absolute. However, due to the possible corrosion in groundwater, a finite container lifetime must be assumed. At present, the container is intended to last for 500 years to 1000 years, which is sufficient for the majority of fission products to decay to stable elements[2]. The activity of the used fuel will decrease very slowly after about 700 years, a result mainly of the decay of actinides with very long half lives.

1.3 CONTAINER ENVIRONMENT

Corrosion degradation of a material is dependent on its environment. To predict with some certainty that the container will satisfy its specified lifetime, a study of the corrosion properties of potential container materials in projected repository environments is necessary. This has required defining the probable vault environmental conditions.

In the disposal vault, the waste package is embedded in a compacted bentonite-sand mixture[3]. Groundwater is expected to flood the vault after its completion. In the Canadian Shield, groundwater is generally saline at depths below 1 km[4]. The most saline brines have salinities exceeding 200 g/L. At depths less than ~1 km, the salinity of groundwater varies considerably. The oxygen concentration in deep groundwater is expected to be <0.1 ppm[1]. However, the oxygen content in the vault before and shortly after flooding will depend on the porosity of the bentonite-sand mixture, which may trap air during backfilling. After flooding, irradiation of groundwater may produce radiolysis products, the amounts of which will depend on the age of the irradiated fuel and the thickness of the container wall. The vault temperature, after closure, will increase as backfilling insulates the repository. With time, less radioactive fission products will be available to generate heat and the vault temperature will decrease. A model of the long-term thermal response of the vault projected a maximum container surface temperature of <150C[5]. Thus, both the physical and chemical properties of a container's immediate environment are specific to the location of the repository, the location of the container within the vault, the disposed time and the thickness of the container wall.

1.4 CONTAINER MATERIAL

Some of the candidate materials under investigation are titanium, copper and carbon steel [6,7,8,9]. Titanium is a corrosion resistant material, protected from corrosive attack in most environments by a surface oxide film. Its failure modes are generally crevice corrosion and hydrogen embrittlement. Both copper and carbon steel are corrosion allowance material. They usually corrode through general wastage and pitting attack. In alkaline environments, carbon steel may also be susceptible to stress corrosion cracking.

The corrosion properties of titanium and the corrosion mechanism of copper as container materials are being studied at Atomic Energy of Canada Limited. Specific environmental effects on the corrosion behaviour of copper are being investigated at Ontario Hydro.

2.0 PROGRAM OBJECTIVE AND APPROACH

The copper corrosion study at Ontario Hydro was aimed at providing information for estimating a corrosion allowance thickness that would satisfy the container's lifetime specification. The main thrust of the project was to obtain copper corrosion rates. Since a set of container environmental conditions cannot be precisely defined, a conservative approach was used to determine the upper bounds of the corrosion rates under probable and hypothetical worst case environments. It was intended that as the copper corrosion mechanism/behaviour and the disposal vault environment become better understood, the corrosion rates or the container corrosion allowance thickness can be better refined. The copper corrosion program consists of two phases:

- Identify parameters that may affect copper's corrosion performance and study the effects of these parameters, and

- Evaluate the localized corrosion performance of copper by studying the effects of various parameters on its pitting and crevice corrosion kinetics.

Ontario Hydro's planned projects for the first phase of the program are completed and projects for the second phase are being initiated.

This report presents findings on the general corrosion behaviour of copper, its corrosion morphology and general corrosion kinetics, and contains two parts:

- a preliminary assessment from available information to define parameters which may affect copper's corrosion rate, and

- experimental results on the effects of irradiation and sulphide ion on copper's corrosion rate in a saline groundwater-bentonite slurry.

3.0 PRELIMINARY ASSESSMENT

In this preliminary assessment, the corrosion behaviour of copper in environments relevant to that of the disposal vault is reviewed. The stability of copper with respect to probable disposal vault conditions is discussed in terms of possible reactions, kinetics, parameters that may affect copper's corrosion rate and the types of localized corrosion that may affect its durability.

Unless otherwise stated, the standard reduction potentials (E°) quoted[10] in this report refer to those of the standard hydrogen electrode scale at 25°C.

3.1 THERMODYNAMICS

Thermodynamic considerations dictate the feasibility of reactions. Since a corrosion reaction results from two half-reactions, these are considered separately.

3.1.1 Cathodic Reactions

To corrode a metallic material, a chemical capable of oxidizing the material must be present at its surface. To be an oxidant, the chemical must have a higher reduction reaction potential than that of the material. In natural waters, hydrogen ion and oxygen are the most common oxidants.

$2H^+ + 2e = H_2$ $E° = 0.00V$

$0_2 + 2H_20 + 4e = 40H^-$ $E° = 0.40V$

Having a more positive standard reduction potential than hydrogen, copper is unaffected by hydrogen ion in the absence of other oxidants, complexing agents and/or sulphide[10].

$Cu^{2+} + 2e = Cu$ $E° = 0.34V$

However, sulphur species are present in most groundwaters and in nature, copper exists mostly as sulphide ore; thus, in the presence of sulphide, hydrogen ion may also be a source of oxidant to copper.

With gamma irradiation, radiolysis of saline water may produce other oxidants[11], such as peroxide and hypochlorite, which can corrode copper.

$H_20_2 + 2H^+ + 2e = 2H_20$ $E° = 1.78V$

$C10^- + H_20 + 2e = C1^- + 20H^-$ $E° = 0.90V$

3.1.2 Anodic Reactions

Because groundwaters of the Canadian Shield are mostly saline and contain sulphur species, which are generally in the form of sulphate, copper's domain of thermodynamic stability in groundwaters in terms of pH and potential may be estimated from pH-potential diagrams calculated from thermodynamic data for aqueous systems containing chloride and/or sulphide[12,13,14].

Though the groundwaters are mostly neutral or slightly alkaline, copper's reactions in acidic pH are also considered here as it may provide insight into its corrosion mechanism and/or kinetics.

In acidic media without chloride or sulphide, copper dissolves as cuprous or cupric ion (Figure 3-1). In natural saline environments, which may contain sulphide species, these reactions are unlikely to occur (Figure 3-2 and 3-3). In these environments, the cupric ion is stable only at low pH and moderately high oxidizing potentials. In slightly acidic to neutral pH, the cupric state exists as copper hydroxychloride, $Cu_2(OH)_3Cl$, at moderate to high oxidizing potentials, or as cupric sulphide at low to moderate potentials. The cuprous state is in the form of cuprous chloride, cuprous chloride complexes and/or cuprous sulphide, dependent on the medium composition, pH and potential.

$Cu_2(OH)_3Cl + OH^- = 2CuO + CL^- + 2H_2O$ $K = 2.24 \times 10^5$

$CuC1 + e = Cu + C1^-$ $E° = 0.14V$

$CuC1 + C1^- = CuC1_2$

$Cu_2S + 2e = 2Cu + S^{2-}$ $E° = -0.93V$

$CuS + 2e = Cu + S^{2-}$ $E° = -0.73V$

In alkaline media, oxidation of copper results in cuprous and/or cupric oxide. Depending on the pH, some amount of cupric oxide may dissolve to give the bicuprite or the cuprite ion. In the presence of sulphide at low potentials, cuprous sulphide may form.

$Cu_2O + H_2O + 2e = 2Cu + 2OH^-$ $\quad E° = -0.36V$

$CuO + H_2O + 2e = Cu + 2OH^-$ $\quad E° = -0.26V$

$CuO + OH^- = HCuO_2^-$ $\quad K = 1.03 \times 10^{-5}$

$CuO + 2(OH)^- = CuO_2^{2-} + H_2O$ $\quad K = 8.1 \times 10^{-5}$

In neutral saline media with sulphide, depending on the system potential, corrosion of copper results in cuprous sulphide, cupric sulphide, copper chloride complexes, cuprous oxide, cupric oxide, and/or copper hydroxychloride.

3.2 KINETICS

Though copper may be thermodynamically unstable in the disposal vault, its durability is dependent upon the corrosion kinetics. As a corrosion reaction is composed of two half-reactions, the kinetics of either half-reaction can control the overall corrosion rate. The kinetics of a half reaction is dependent on its charge transfer rate constant and the concentrations of reactants and/or products at the corroding surface. The charge transfer rate constant is dependent on the system potential and temperature; the surface concentrations of reactants or products are dependent on their bulk concentrations, their mode of mass transport to or away from the surface and the rates of other reactions in which they may be involved. In general, increasing the potential or the temperature increases the half-reaction rate until the depletion of reactants or the accumulation of products at the surface becomes rate limiting.

The following reviews the kinetics of the half-reactions of copper corrosion in environments that are relevant to those of the disposal vault and the influences of the various parameters on their reaction rates.

3.2.1 Copper Dissolution

In the anodic half of the copper corrosion reaction, without considering any adsorption phenomenon, the first step is oxidation of copper to the copper (I) state. In an acidic medium, the copper(I) state exists as cuprous ion, which may be further oxidized or disproportionated to cupric ion[15].

$Cu^+ + e = Cu$ $\quad E° = 0.52V$

$Cu^{2+} + e = Cu^+$ $\quad E° = 0.16V$

$2Cu^+ = Cu + Cu^{2+}$ $\quad K = (Cu^{2+})/(Cu^+)^2 = 1 \times 10^6$

The transfer of electrons between copper, cuprous ion, and cupric ion is a fast process. This can be deduced from electrode kinetic studies of copper in acidic cupric sulphate solutions[15,16,17,18]. In these studies, the cupric ion/copper half reaction was shown to be quasi-reversible having a relatively large exchange current density ranging from 1 to 80 mA/sq. cm. The reaction proceeds with two 1-electron steps and the rate determining step was shown to be the slower cupric ion/cuprous ion reaction[19,20]. At the open circuit potential, an additional step, the desorption of the cuprous ion, was postulated to be slower[20,21]. This implies that the cuprous ion/copper couple is reversible and that the standard heterogeneous rate constant

for the dissolution of copper to cuprous ion is large. Thus, the rate of the anodic half of the copper corrosion reaction can only be limited by the rates of mass transport of the cuprous or cupric ion away from the surface and/or the rate of simultaneous or following chemical reactions which involve these ions.

In a neutral or an alkaline environment the primary corrosion product is cuprous oxide. Depending on the system potential, the cuprous oxide may be further oxidized to cupric oxide. The solubility product of cuprous oxide, ~1 x 10^{-14}, and cupric oxide, ~1 x 10^{-19}, are very small[22] and the oxides are deposited on copper's surface. The formation of a cuprous oxide film on copper's surface is via a dissolution-precipitation mechanism and the rate determining step was shown to be the dissolution of a soluble copper (I) intermediate[23,24,25,26]. With an oxide film, potentiodynamic polarization showed that copper becomes passive[27,28]. Since cuprous oxide is a p-type semiconductor, presumably, further oxide growth is controlled by migration of positive ions through the layer. In addition, the cuprous oxide film/layer was postulated to have a porous structure[29]. Mass transport through pores/fissures may also affect the anodic reaction rate.

3.2.2 Oxygen Reduction

In the cathodic half of the corrosion reaction, in the absence of sulphide and/or radiation, the most probable oxidant is oxygen. In aerated acidic saline solutions at room temperature, the corrosion potential of copper is not sufficiently negative for the reduction of oxygen to be mass transport controlled [30,31]; it is within the potential region where the reduction of oxygen is controlled by activation kinetics. Further, in an acidic sulphate solution, it was suggested that a surface film on copper, which was composed of oxygen reduction intermediate, products and adsorbed sulphate, could result in an additional overpotential for the reduction of oxygen[32], which slows down its reaction rate. Thus, in an acidic saline solution with an ample supply of oxygen, the cathodic reaction is controlled by activation kinetics. However, with a decreasing rate of supply of oxygen, the potential at which oxygen reduction becomes mass transport limited will shift anodically[33] and depending on the corrosion potential, the cathodic reaction could become mass transport controlled.

There is no available information on the reduction kinetics of oxygen on copper in neutral or alkaline environments.

3.2.3 Diffusion

Without more experimental information on the rate determining step of copper corrosion in neutral or slightly alkaline media and without knowing the corrosion potential of copper in the disposal vault, one may assume the fastest corrosion rate which copper could achieve with oxygen as the oxidant is controlled by mass transport processes.

In a reflooded disposal vault, under steady-state transport conditions, the fastest mode of mass transport is diffusion. For corrosion of copper to copper(I) controlled by diffusion of a reactant or a product in a diffusion layer with a fixed thickness, the corrosion rate, in cm/a, is derived in Appendix 1 as:

$$R = (2.247E8)n_L(D/\delta)C$$

where:

n_L = number of electrons transferred in the diffusion limited half reaction

D = diffusion coefficient in cm^2/s

δ = fixed diffusion layer thickness in cm, and

C = concentration in moles/cm^3

By assuming that the groundwater flow rate in the geologic formation is comparatively faster than the rate of diffusion in the buffer material, the maximum thickness of the diffusion layer is fixed by the thickness of the buffer material. To illustrate calculation of corrosion rates after the establishment of a fixed diffusion layer, the buffer material thickness is arbitrarily set at 25 cm, the diffusion coefficient at 1×10^{-6} cm^2/s and concentration at 0.1 ppm. If the corrosion reaction is controlled by the diffusion of oxygen to the corroding surface, the long term corrosion rate is estimated to be less than 1.2×10^{-3} µm/a. When diffusion of copper(I) away from copper's surface is rate limiting, the rate is less than 1.5×10^{-4} µm/a. Thus, with oxygen as oxidant, in the absence of sulphide, radiation, localized corrosion and/or any other factor which may enhance copper corrosion, a container with a thickness of 1.5 cm, which includes a safety or error factor of 10, should adequately last for 10^6 years without failure by corrosion.

3.3 OTHER RATE CONTROLLING PARAMETERS

Other factors which may affect the corrosion rate of copper include salinity, temperature, sulphide and/or irradiation.

3.3.1 Salinity

Because the chloride content in groundwaters varies over a wide range, the salinity discussed here is concerned mainly with chloride ion. It should be noted that, in an open system, increasing salt concentration generally decreases oxygen's solubility and, if a corrosion reaction is controlled by oxygen reduction kinetics, an effect of increasing the salinity is decreasing the corrsion rate.

In acidic chloride solutions, copper corrodes to form solid cuprous chloride on its surface. When a sufficient amount of chloride is present to completely cover copper's surface with cuprous chloride, the corrosion rate will decrease[30]. With increasing chloride concentration, copper and/or cuprous chloride reacts to form soluble cuprous chloride complexes. Copper's surface is exposed and the corrosion rate will increase. In saline solutions, the anodic reaction for copper dissolution was shown by electrochemical methods to be controlled by mass transport of the chloride complexes away from copper's surface[30,31,34,35]. The anodic current is dependent on the surface concentration of cuprous chloride complexes, which, in turn depends on chloride concentration[34,35]. It follows that if the corrosion kinetics is controlled by the anodic reaction, increasing chloride concentration above a certain threshold for the formation of the complexes should increase the corrosion rate. However, Robertson et-al[36] showed experimentally that the dependence of copper corrosion rate on salinity is complicated. In air saturated, continuously refreshed solutions at pH=2, increasing chloride or sulphate concentration decreased the copper corrosion rate, whereas at pH=6, increasing chloride concentration increased the corrosion rate and increasing sulphate concentration had little effect on copper's corrosion performance.

In a synthetic groundwater-bentonite slurry, experiments performed at Ontario Hydro[37] showed that, at 150°C, for a chloride concentration varying from 5 ppm to 50,000 ppm, salinity had no significant effect on copper corrosion rate. At 75°C, any significant effect was not apparent because of the scatter in results or experimental uncertainty.

3.3.2 Temperature

It is generally known in chemical kinetics that increasing temperature increases the rates of reactions which have a single step mechanism. In general, the rate is an exponential function of temperature. Further, for a diffusion controlled corrosion reaction, the diffusion coefficient increases as temperature increases and thus, the corrosion rate increases.

In a saline solution at a temperature in a range 25°C to 175°C, the anodic reaction for copper dissolution has a temperature coefficient, dE°/dT, with a negative value[35]. The anodic current-potential curve shifts cathodically as temperature increases. Thus, provided the cathodic reaction rate does not decrease, increasing temperature increases copper's corrosion rate. In an aerated synthetic sea water with a pH=8.2, for times less than 72 hours, increase in temperature from 25C to 60C did increase the corrosion rate of copper, but for longer times, the corrosion rate decreased as temperature increased [38]. The decrease in corrosion rate was attributed to the formation of cuprous oxide and could also be partly due to the decrease in oxygen solubility as temperature was increased. However, Robertson at-el[36] observed that in a pH=6 saline solution which was either saturated with air or fixed with a constant oxygen concentration, the corrosion rate of copper peaked in the temperature range 71°C-77°C. At pH=2, the rate similarly went through a maximum in open systems but followed the general exponential dependency on temperature in systems with a constant oxygen concentration.

Experiments performed at Ontario Hydro in a synthetic saline groundwater-bentonite slurry showed that, in aerated slurries, the corrosion rate of copper peaked in the temperature range 70°C - 80°C, but in deaeated slurries, temperature has no apparently significant effect on the corrosion rate of copper[37].

3.3.3 Sulphide

In the presence of sulphide, the corrosion rate of copper may be enhanced. B.C. Syrett[39] studied the effects of sulphide on copper's corrosion rate at two levels of oxygen concentrations. In waters with a low oxygen concentration, 29 ppb to 60 ppb, sulphide had insignificant effect on copper's corrosion rate. At an oxygen concentration of ~870 ppb, the presence of sulphide increased the corrosion rate of copper by at least 10 times. He postulated that at any fixed oxygen concentration, copper's corrosion rate will increase as sulphide concentration increased up to a critical sulphide concentration, above which, any increase in sulphide concentration will have no significant effect on copper's corrosion rate.

There is no available information on the effects of sulphide on copper's corrosion rate in saline waters.

3.3.4 Radiolysis

The radiation chemistry of brine has been reviewed and some of the yield values of the radiolysis products have been determined/collected by Jenks[9]. However, there is still a lack of information on the yield (G values) of radiolysis products in saline groundwater at high temperatures. Also, little is known about the effects of radiolysis on the corrosion rate of copper. In radiolysis, equal amount of oxidants and reductants are produced. In a closed system, this will not change the system potential. However, differential migration of reductants and oxidants may result in non-uniform corrosion.

3.4 LOCALIZED CORROSION

3.4.1 Pitting

Besides uniform corrosion, pitting has been observed on copper in fresh and sea waters[40], in solutions

containing sulphide[41] and in soils[42]. Fresh waters in which copper pits usually contain 10-12 ppm of oxygen and up to several hundred ppm of chloride. City waters may also contain residual chlorine from water treatment. The sea waters contain sulphide. The soils in which copper pitted varied from acidic to alkaline, silt to clay, and relatively dry to water-saturated.

In describing the susceptibility of a metallic material to pitting attack, pitting potential is a term commonly used. It is defined here as a potential of the material below which the occurrence of pitting is a rare event. If a material attains a potential above its pitting potential in a particular environment, pitting usually occurs, or if a material has a low pitting potential in a particular environment, the material when exposed to that environment will be prone to pitting attack. In aerated fresh waters and city waters, the pitting potential of copper was ~0.015V vs a saturate calomel electrode[43,44,45]. In deaerated saline waters, measurements of pitting potential are scattered over a wide potential range. At pH=9, at a temperature in a range 15°C-50°C, the pitting potential varied between 0.4V to 0.75V[46,47]. At neutral pH to pH=9, the pitting potential was -0.15V at 15°C[30].

The morphology of pits depends on the hardness of the water[40]. In hard or moderately hard waters with a high sulphate content, the pits are large and hemispherical. In soft waters at a temperature greater than 60°C, the pits are narrow and deep. The pits usually contain cuprous oxide and are often covered with basic copper carbonate and/or sulphate.

In solutions containing 0.01M of sulphide and 0.1M of hydroxide, the pitting potential was -0.74V[41]. The pitting potential shifted 60 mV in the negative direction per decade increase in sulphide concentration from 0.001M to 0.01M.

In various soils for periods of up to 14 years, the average general corrosion rate of copper was measured[42] ranging from <1 µm/a to 30 µm/a and the pitting factor (a ratio of pit depth to average corrosion penetration) 1.1 to 24.

The wide range of environments in which copper can be pitted suggests that pitting is not a rare phenomenon with copper. Further, the pitting potential suggests that the probability of pitting on copper is highest in environments containing sulphide.

3.4.2 Stress Corrosion Cracking

Stress corrosion cracking of copper has been reported in the literature in acetate solutions[48]. Nitrite may also stress corrosion crack copper at a concentration greater than 1mM and at a potential greater than 0.3 V vs SCE[49]. Chloride and sulphate have no effect on the stress corrosion susceptibility of copper. It is not expected that copper will stress corrosion crack in the disposal vault.

4.0 EXPERIMENTAL

4.1 TEST SAMPLE

The test material was oxygen-free high conductivity copper (UNS C10200). The copper corrosion coupons were fabricated as blocks, each with a surface area of ~5 sq. cm. and a surface finish of 1µm. The edges of the block were lightly rounded to avoid preferential corrosion at sharp edges. The surface finish was examined through an optical microscope and any coupon with an unsatisfactory finish was re-polished. The polished coupons were ultrasonically cleaned with isopropyl alcohol, then with deionized water, and stored in a desiccator before use. At least 3 coupons were used for each experimental run.

4.2 TEST ENVIRONMENT

The test medium was a synthetic saline groundwater-Na bentonite slurry mixed in a ratio of 4 ml of solution per g of clay. Table 4-1 gives the nominal composition of the saline groundwater, which approximated the compositions of groundwater samples taken from the Lac Du Bonnet Batholith at a depth of 455m and was designated as WN1[50]. Appendix 2 gives the procedure for the preparation of the WN1 solution.

TABLE 4-1

NOMINAL WN1 SOLUTION COMPOSITION (ppm)

Na^+	Ca^{2+}	Mg^{2+}	Cl^-	SO_4^{2-}	HCO_3^-
1900	2100	60	6500	1000	70

The pH of the solution was ~7.0.

The pH of the slurry was stable during all experiments; a variation of ± 0.5 of its original value was recorded.

To test the effects of oxygen, the medium was either exposed to air or deaerated with nitrogen. In deaerated experiments, the medium was purged with moist nitrogen for at least 48 hours before the introduction of the test samples and, afterwards, was blanketed with nitrogen. The oxygen content of the deaerated medium measured at room temperature by an oxygen electrode (Orion Research 97-08) was less than 0.1 mg per L of slurry.

When testing the effects of sulphide, the test medium contained an initial sulphide concentration of 10 mg per litre of slurry. In the experiments performed without irradiation, additional sulphide, in an amount of 10 mg per litre of slurry was added daily to the test medium. This additional sulphide replenished any loss in sulphide through oxidation or reaction with copper and created an environment which may represent as a worst case scenario in the disposal vault. Sulphide was added to the slurry as a concentrated solution of sodium sulphide via a calibrated hypodermic syringe. The concentrated sulphide stock solution was kept under moist nitrogen to prevent oxidation. Its sulphide content was analyzed periodically by titration with lead perclorate using ascorbic acid as an anti-oxidant and an ORION Research sulphide ion selective electrode as an end point indicating sensor. The procedure for the analysis was given in the instruction manual for the sulphide electrode.

When testing the effects of radiation, the test medium was deaerated for at-least 48 hours before the start of the experiment and irradiated at a rate of ~150 Rad/h during the experiment. The experiments were performed beside 7 years old Candu irradiated nuclear fuel bundles stored in the Auxiliary Irradiated Fuel Bay at the Pickering Nuclear Generating Station. The radiation rate was measured using a high range γ-meter, which was calibrated against a Cs-137 and/or a Co-60 source. Appendix 3 details the location and the equipment of the experiment.

The temperature of the experiments was either 75°C or 150°C. Heat was supplied by either thermostatic water baths or heating tapes and heating mantles controlled by temperature controllers. The temperature was maintained to within ±1°C.

At 75°C, the test medium was contained in a 1L glass corrosion cell with cold fingers to condense water

vapour. Any solution lost due to vaporization, which occurred very slowly, was made up with deionized water. At 150°C and for all experiments performed under irradiation, the test medium was contained in a 850 mL glass lined Inconel autoclave.

4.3 TEST DURATION

The test duration lasted from two months to approximately a year.

4.4 ANALYTICAL TECHNIQUES

4.4.1 Polarization Resistance

The progress of corrosion was monitored by polarization resistance using a potentiostat with a conventional three electrode arrangement. The electrodes were similar copper coupons. Current-potential data were measured between ±25 mV of the corrosion potential. A numerical method[51] and closed form analytical equations[52] were used to calculate corrosion rate directly from the current-potential data. However, often, a solution could not be obtained, and when a corrosion rate was calculated, its value was often smaller than that obtained from the weight loss method. This was probably because the mathematical methods require very accurate inputs and the experimental data were not sufficiently accurate due to corrosion potential variations during measurement and due to the corrosion products formed on the coupon which increased its resistance. Thus, the current-potential data were used only to graphically estimate resistance for use to indicate the corrosion rate-time trend and not to calculate corrosion rate.

4.4.2 Potential Measurement

In some experiments, the copper potential was followed via a salt bridge with a silver-silver chloride electrode placed at room temperature.

4.4.3 Optical Method

An optical microscope and/or a scanning electron microscope (SEM) were used to examine the morphology of an exposed coupon before and after removal of corrosion products. The compositions and identifications of corrosion products were determined by energy dispersive X-ray spectroscopy (EDXS) and/or X-ray diffraction.

4.4.4 Descaling

Corrosion rates were obtained by the weight loss method. Loose corrosion products were scraped off with a plastic spatula. Adherent products were removed according to the ASTM G1-72 procedure but with a more diluted cleaning solution, which contained, in proportion, 50 mL of conc. hydrochloric acid, 10 mL of conc. sulphuric acid and 540 mL of water. The coupons were dipped in the solution for 30 s. If corrosion products were not completely removed, the 30 s. dip was repeated for up to a total time of 3 minutes. Afterwards, the coupons were rinsed with deionized water and any remaining products were scraped off with a plastic spatula. Controlled experiments using fresh coupons showed the cleaning process would not cause any significant weight loss nor any pitting.

4.4.5 Pit Depth Measurement

Pit depth was measured by a difference in reading on a calibrated focusing dial of an optical microscope by focusing the top and bottom of a pit. The precision of the method was ±1 μm.

5.0 RESULTS

5.1 CORROSION RATE-TIME TREND

Figures 5-1, 5-2, 5-3 and 5-4 show the typical corrosion rate-time trends for copper. These are plotted as the reciprocal of resistance, which, under ideal conditions, is approximately proportional to the instantaneous corrosion rate. Except for trends in aerated slurries at 75°C, the corrosion rate-time trends of copper were similar. In the first 10 to 20 days, the rate decreased gradually and after a month, became stable or slowly decreased further. In aerated slurries at 75°C, the rate similarly decreased for the first 10 to 20 days, but during the next 10 to 20 days, the trend reversed its direction and increased before it decreased again in slurries without sulphide or stabilized in slurries with sulphide.

5.2 CORROSION RATE

Table 5-1 gives the average corrosion rates of copper based on weight loss.

TABLE 5-1

COPPER CORROSION RATES IN A GROUNDWATER-BENTONITE SLURRY
(μm/a)

TEMP	SLURRY	WN1-S	WN1	DURATION (months)
75°C	Dearated	14.8 ± 3.0 (4)*	1.37 ± 0.39 (3)	10 - 15
	Aerated	79.9 ± 23.2 (4)	54.1 (1)	10 - 15
	Dearated-R	6.13 ± 1.87(7)	7.41 ± 5.66 (6)	~9
150°C	Dearated	17.1 ± 1.7 (5)	23.5 ± 6.2 (5)	2 - 6
	Aerated	86.4 ± 7.1 (7)	15.4 ± 8.7 (8)	2 - 6
	Dearated-R	9.75 ± 7.25(6)	6.08 ± 5.27 (7)	~5

Note:

* - Rate = Average ± 1 standard deviation (number of samples)

Deaerated-R - denotes deaerated slurries under irradiation

WN1 - a synthetic saline groundwater; see Table 4-1 for composition.

WN1-S - represents WN1 with an initial sulphide content of 10mg/L. For slurries without irradiation, sulphide (10 mg/L) was added daily.

5.2.1 Effects of Oxygen

The corrosion rate of copper was generally higher in aerated slurries than in deaerated slurries. An exception was in test media without sulphide at 150°C where a higher oxygen content resulted in a lower rate.

5.2.2 Effects of Temperature

In slurries with sulphide, increasing their temperature from 75°C to 150°C showed a slight increase in copper's corrosion rate.

In slurries without sulphide, oxidant content had an influence on the effect of temperature on the corrosion rate of copper. In media with a low oxidant content, the deaerated slurries, an increase in temperature increased the corrosion rate, whereas in aerated slurries and in slurries under irradiation, an increase in temperature decreased the corrosion rate.

5.2.3 Effects of Sulphide

The presence of sulphide generally raised copper's corrosion rate. There were exceptions: in deaerated slurries at 150°C, and in slurries under irradiation at 75°C, the rates were approximately the same or slightly lower.

5.2.4 Effects of Radiolysis

Irradiation generally lowered copper's corrosion rate except at 75°C in the absence of sulphide, the rate was higher.

5.3 CORROSION PRODUCT

The exposed coupons were usually covered with loose deposits and corrosion products as spots, patches, or powdery or compact film on top of a layer of more adherent but porous corrosion product. Table 5-2 gives the colour/appearance of the exposed coupons. Table 5-3 identifies the corrosion products.

TABLE 5-2

APPEARANCE OF COPPER COUPONS AFTER EXPOSURE TO WN1-GROUNDWATER-BENTONITE SLURRY

SLURRY	DEAERATED	AERATED	DEAERATED-S	AERATED-S
75°C	brn-red	brn-blk	gry-blk	gry-blk
150°C	red with grn & blk spots	red with grn & blk spots	gry-blk	gry-blk
75°C-R	brn-red with wh & bl-grn spots	NT	gry-blk with wh & bl-grn spots	NT

150°C-R	brn-red with wh & bl-grn spots	NT	gry-blk with wh & red spots	NT

Note: bl=blue, blk=black, brn=brown, grn=green, gry=grey, wh=white

WN1 - see Table 4-1 for composition
S - denotes the slurry contained sulphide
R - denotes the slurry was under irradiation
NT - no experiments performed

TABLE 5-3

CORROSION PRODUCTS AND DEPOSITS ON COPPER AFTER EXPOSURE TO WN1 GROUNDWATER-BENTONITE SLURRY

SLURRY	DEAERATED	AERATED	DEAERATED-S	AERATED-S
75°C	NA	NA	Cu_2S	Cu_2S
150°C	Cu_2O, CuO $Cu_2C1(OH)_3$, $CaCO_3$	Cu_2O, CuO, $Cu_2C1(OH)_3$	Cu_2S	Cu_2S, Cu_2O
75°C-R/ 150°C-R	Cu_2O, $Cu_2C1(OH)_3$, $CaCO_3$	NT	Cu_2O, $Cu_2C1(OH)_3$ $CaCO_3$	NT

Note: WN1 - a synthetic saline groundwater, see Table 4-1 for composition
S - denotes the slurry contained sulphide
R - denotes the slurry was under irradiation
NA - no analysis was performed
NT - no experiment was performed

The corrosion product on coupons exposed to deaerated and aerated slurries at 75°C was not analyzed because the former coupons had an insufficient amount of collectable product and the latter were too few in number to allow for product collection for analysis. However, the corrosion products had the colour of cuprous oxide.

In slurries not containing sulphide, the corrosion product was cuprous oxide and/or cupric oxide. The cuprous oxide was identified as cuprite (Figure 5-5a), and the cupric oxide was tenorite. Some cupric oxide was in the form of copper hydroxyl chloride as $Cu_2C1(OH)_3$, and a minute amount as $Cu_7C1_4(OH)_{10}.H_2O$. In removing the corrosion products for analysis, the following appearances of the products were noted. The green product (hydroxyl chloride) was found generally as loose deposits/layer on top of a patch of

black product (cupric oxide) or occasionally on the reddish brown layer (cuprous oxide), which adhered firmly on copper's surface. Though the products grown in deaerated and aerated slurries at 150°C were similar, their appearances/morphologies were, in general, slightly different. In deaerated slurries, there were often two layers of black products, a relatively soft outer layer and a hard inner layer, which adhered on the reddish brown oxide. In aerated slurries, the black product formed only a single layer which spalled in some areas. The reddish brown layer grown in aerated slurries was generally thicker than that grown in deaerated slurries.

In slurries containing an initial amount of sulphide under irradiation, the corrosion products were cuprous oxide and copper hydroxyl chloride (Figure 5-5b). Copper sulphide was not detected.

Calcium carbonate was frequently deposited in small amounts on top of copper oxides in deaerated slurries at 150°C and in slurries under irradiation (Figure 5-6A). Often, the layer of cuprous oxide on copper's surface was porous (Figure 5-6b).

In slurries with a daily addition of sulphide, the corrosion product was cuprous sulphide. In aerated slurries at 150°C, cuprous oxide was also detected. The cuprous sulphide was chalcocite. Some amount of djurlerite and gerrite were also identified. The cuprous sulphide consisted of two layers. The upper layer was compact and the inner layer porous (Figure 5-7, 5-8). The upper layer could be peeled off from the inner layer, but the inner layer was adherent as it penetrated the generally roughened surface of copper (Figure 5-9).

5.4 CORROSION MORPHOLOGY

The copper surface had a smooth appearance after exposure in deaerated slurries without sulphide. However, under magnification, a slightly roughened surface and the occasional very shallow pits were revealed (Figure 5-10a). In contrast, after exposure in sulphide media, the surface was rough (Figure 5-10b) and the pits were much deeper and more numerous (Figure 5-11, 5-12). In most areas, it appeared that smaller pits had coalesced to form a bigger but shallower pit. The high density of these pits resulted in a rough surface appearance. However, there are small areas where the surface was relatively smooth with a few deeper pits.

In slurries under irradiation, a high density of very small pits was observed. In areas where the adherent porous layer of corrosion product was thin, some pits opened through the layer and could be observed microscopically before descaling (Figure 5-13). After descaling, because of the small size of the pits, copper's surface appeared smooth visually. The pits were actually of various sizes (Figure 5-14, 5-15), and some appeared to have been initiated at grain boundaries. In most pits, crystallographic planes could be clearly seen (Figure 5-16), and in a few small areas, intergranular corrosion was indeed observed (Figure 5-17).

5.5 PITTING RATE

Table 5-4 gives the maximum pitting rate which was calculated by dividing the depth of the deepest pit with the exposed time and does not represent the fastest instantaneous growth rate at the end of exposure. It must be noted that the deepest pit generated in a particular environment might not have been located.

TABLE 5-4

MAXIMUM PITTING RATE OF COPPER IN A GROUNDWATER-BENTONITE SLURRY

(mm/a)

TEMP	SLURRY	WN1-S	WN1
75°C	Deaerated	0.57	0.014
	Aerated	1.2	0.087
	Deaerated-R	0.039	0.064
150°C	Deaerated	0.88	0.16
	Aerated	0.32	0.92
	Deaerated-R	0.016	0.088

Note: WN1 - a synthetic saline groundwater; see Table 4-1 for composition.
S - denotes the slurry contained sulphide (10 mg/L).
R - denotes the slurry was under irradiation at 150 rad/h.

In general, pits were deeper in aerated slurries than in deaerated slurries for a comparable exposure time. At 75°C and without irradiation, the presence of sulphide produced deeper pits. At 150°C, the effect of sulphide on pitting was not obvious. Irradiation appeared to have a beneficial effect on pitting, except in slurries without sulphide at 75°C where irradiation generated deeper pits.

5.6 CORROSION POTENTIAL

The potential of copper was monitored only in slurries without irradiation at 75°C. The reference electrode was a Ag/AgC1 electrode at room temperature.

In deaerated slurries without sulphide, the potential stabilized after a month at around -0.28 volt. In aerated slurries, the potential fluctuated around -0.22 volt for a while and gradually decreased to -0.28 volt after three months.

In slurries with sulphide, stable potential was achieved after three months. Aerated slurries gave a potential of -0.49 volt and deaerated slurries -0.88 volt.

6.0 DISCUSSION

It is apparent from the experimental results that oxidant content (oxygen, bisulphide, hypochlorite) had the greatest influence on the corrosion behaviour of copper in saline groundwater-bentonite slurries. It exerted its influence by supporting the cathodic half of the corrosion reaction and by affecting the protectiveness of the corrosion products. In general, an increase in oxidant concentration increased the corrosion rate. In the case of slurries without sulphide at 150°C, an increase in oxidant content slightly lowered the corrosion rate, which was probably a result of variations of the protectiveness of the corrosion product. The layer of corrosion product immediately on the copper surface was porous. Occasionally, this same product (cuprous oxide or sulphide) would acquire a dual structure having a compact layer formed on top of the

porous layer. The formation of a more protective layer would impede the corrosion rate. The observation of a slightly lower corrosion rate in aerated slurries than in deaerated slurries at 150°C but not at 75°C suggests that there may be some combinations of oxidant and temperature levels above which might promote the formation of the compact layer. This postulation is consistent with an earlier observation that in a pH=6 solution with a constant oxygen concentration, copper's corrosion rate peaked in the range 70°C-80°C[36], and with a deduction that at any one oxygen concentration, there is a corresponding threshold sulphide level above which copper's corrosion rate would remain approximately the same or increase very slowly[39]. The influence of time on the formation of the compact layer is not clear. The present data is insufficient for deducing whether a compact layer will form with time. Very long term experiments with periodic removal of samples for corrosion product examination would clarify this.

The porosity of the corrosion product might also have been responsible for copper's corrosion morphology. Though the spacial relationship between the pores and copper's microstructure has not been examined, it or the formation mechanism might have resulted in the initiation of intergranular corrosion. Also, pores, similar to crevices, are favourite locations for forming concentration cells. The porosity of the corrosion product might have resulted in the high density of tiny pits. With time, the tiny pits probably coalesced to form bigger but shallower pits resulting in a generally roughened surface appearance.

The corrosion products in both aerated and deaerated neutral saline solutions have been suggested as cuprous chloride complexes in earlier studies[30,31]. Results from these studies indicated that copper's dissolution rate was controlled by mass transport of the soluble complexes away from the corroding surface. However, in the present study, the corroded coupons were covered with insoluble copper oxides and salinity did not apparently affect copper's corrosion rate[53]. Though the experimental temperature and medium for this and the earlier studies were different, the major differences are that the earlier works used hydrodynamic methods and their experimental times were short. When hydrodynamic techniques were used, the natural surface chemistry was disturbed and could have prevented oxide deposition. Also, the present results have shown that a pseudo-steady state was achieved at least after a month for deaerated slurries without sulphide. The corrosion product and corrosion process could have changed with time and a short duration experiment might not have been able to detect such changes in mechanism.

The pseudo-steady state corrosion potential of copper in slurries without sulphide at 75°C was -0.28 volt vs Ag/AgC1. Current-potential curves have shown that oxygen reduction on copper in a quiescent, air saturated saline solution becomes diffusion limited below -0.28 volt vs SCE at 25°C[33]. With a smaller oxygen concentration, it is probable that the oxygen reduction reaction in the present study was diffusion limited (Figure 6-1), unless the reduction on an oxide covered surface required a large additional overpotential. In media containing sulphide at 75°C, the corrosion potentials were -0.49 volt and -0.88 volt vs Ag/AgC1 respectively for aerated and deaerated slurries. These potentials were more negative than the hydrogen reduction potential and hydrogen ion or the bisulphide ion, besides oxygen, were the oxidant in the cathodic process[53]. There is not a mechanistic study on the corrosion process of copper in media containing sulphide nor in media under irradiation.

The corrosion rate of copper determined in deaerated slurries without sulphide at 75°C was 1.37 ± 0.39 µm/a. It agrees well with the result of a similar set of experiments reported earlier[53]. However, the rate is two orders of magnitude higher than that calculated from the integrated Cottrell equation for a diffusion limited oxygen reduction controlled corrosion reaction/Appendix 1/. This could probably be due to an initial corrosion mechanism which was more complicated and produced a higher rate than that of the diffusion limited model or to the combination of a minute weight loss and an insufficiently long duration of exposure which resulted in a much higher average corrosion rate. The corrosion rates obtained in other experimental conditions were less precise because of the nature of the non-uniform corrosion. Further long duration experiments may provide more accurate results.

With regard to pitting, it is not certain at present whether some pits will continue to grow and propagate, and if some do, their statistical significance may have to be assessed. Further study will be required to clarify this.

7.0 CONCLUSION

Without more long term experimental data or a more accurate mathematical model for the copper corrosion process, the corrosion rate of copper in the disposal vault may be assumed to be within bounds of the corrosion rates determined here under the various presumed vault conditions. In a sulphide free environment at 75°C without any radiolysis effects, the long term copper corrosion rate was determined to be less than 2 µm/a, with radiolysis, the rate was less than 10 µm/a and in an environment equilibrated with air as in an open system, the rate was approximately 50 µm/a. With sulphide, the maximum rate was approximately 80 µm/a.

With regard to the corrosion behaviour of copper, the following are some specific observations and deductions:

1. An increase in oxidant content generally increases the corrosion rate of copper whereas salinity has no apparent effect.

2. Radiolysis has a generally beneficial effect on the corrosion of copper.

3. Increase in temperature or increase in oxidant level generally increase copper's corrosion rate unless the surface is covered with a compact layer of corrosion product.

4. The adjacent layer of corrosion product on copper's surface is porous. The layer on top of the porous layer in a multi–layered corrosion product is usually compact.

5. There may be some combinations of temperature and oxidant content levels at which conditions are favourable for the production of an outer compact layer of corrosion product.

6. A badly corroded surface of copper has a generally roughened appearance, the majority of which is a result of the coalescence of pits.

7. Though most pits coalesced and resulted in the general wastage of copper, the present data are insufficient to determine whether some pits will continue to grow and propagate. Further study will be required to determine the pitting rate trend.

8.0 ACKNOWLEDGEMENT

Identification of corrosion product was performed by Ontario Hydro Research's Analytical Services. Lloyd Chee's tireless effort in performing the experiments and the cooperation of the Pickering NGS Fuel Handling group in conducting the radiolysis experiments are greatly appreciated. David Shoesmith's review of the report and helpful suggestions is gratefully acknowledged.

Recomended by:

P.C. Lichtenberger
Supervising Scientist
Corrosion & Tritium
Technology Section
Metallurgical Research Dept

Submitted by:

K.W. Lam
Engineer
Corrosion & Tritium
Technology Section
Metallurgical Research Dept

Approved by:

J. Brown
Manager
Metallurgical Research Dept

Reviewed by:

J.D. Chadha
Area Co-ordinator
AECL Technical Assistance Program

REFERENCES

1. The Swedish Corrosion Institute, "Handling and Final Storage of Unreprocessed Spent Nuclear Fuel", Volume II, Stockholm, Sweden, 1978.

2. Atomic Energy of Canada Limited, "Management of Radioactive Fuel Wastes: The Canadian *Disposal Program", J. Boulon (Editor), AECL–6314, 1978.*

3. D.A. Dixon, M.N. Gray and A.W. Thomas, Engineering Geology 21, 247 (1985).

4. P. Fritz and S.K. Frape, Chemical Geology 36, 179 (1982).

5. S.A. Mayman, R.G. Charlwood and J.L. Ratigan, "Long–term Thermal Response of a CANDU Fuel Disposal Vault", Atomic Energy of Canada Limited Report, TR–134, 1980.

6. K. Nuttall and V.F. Urbanic, "An Assessment of Materials for Nuclear Fuel Immobilization Containers", Atomic Energy of Canada Limited Report, AECL–6440, 1981.

7. The Swedish Corrosion Institute, "Copper as Cannister Material for Unreprocessed Nuclear Waste – Evaluation with Respect to Corrosion", KBS report–90, 1978.

8. M.A. Molecke, J.A. Ruppen and R.B. Diegle, "Materials for High Level Waste Cannister/Overpacks in Salt Formations", Sandia National Laboratories Report, SAND–82–0429, 1982.

9. G.P. Marsh and K.J. Taylor, Corros. Sci. 28, 289 (1988).

10. W.M. Latimer, "Oxidation Potentials", Prentice–Hall, New York, 1956.

    M.S. Antelman, "The Encylopedia of Chemical Electrode Potentials", Plenum Press, New York, 1982.

11. G.H. Jenks, "Radiolysis and Hydrolysis in Salt–Mine–Brines", Oak Ridge National Laboratory Report, ORNL–TM–3717, 1972.

    G.H. Jenks, "Review of Information on the Radiation Chemistry of Materials Around Waste Canisters in Salt and Assessment of the Need for Additional Experimental Information", Oak Ridge National Laboratory Report, ORNL–5607, 1980.

    G.H. Jenks and J.R. Walton, "Radiation Chemistry of Salt–mine Brines and Hydrates", Oak Ridge National Laboratory Report, ORNL–5726, 1981.

12. M. Pourbaix, Corrosion 25, 267–281 (1969).

13. E.D. Verink, Jr., "Applications of Electrochemical Techniques in the Development of Alloys for Corrosive Service", in "Electrochemical Techniques for Corrosion", National Association of Corrosion Engineers, Texas, 1977.

14. Electric Power Research Institute, "Computer–Calculated Potential pH Diagrams to 300°C, EPRI NP-3137, Volume 2, 1983.

15. J. O'M. Bockris and B.E. Conway, J. Chem. Phys. 28, 707 (1958).

16. E. Mattson and J. O'M. Bockris, Trans. Faraday Soc. 58, 1586 (1962).

17. I.M. Pearson and G.F. Schrader, Electrochim. Acta 13, 2021 (1968).

18. Z.D. Stankovic, J. Electrochem. Soc. 128, 1862 (1981).

19. I.R. Burrows, J.A. Harrison and J. Thompson, J. Electroanal. Chem. 58, 241 (1975).

20. O.R. Brown and H.R. Thirsk, Electrochim. Acta 10, 383 (1965).

21. G. Demedts and A.P. Peteghem, Corros. Sci. 18, 1041 (1978).

22. L.C. Sillen and A.E. Martell, "Stability Constants", The Chemical Society, Special Publication No. 17, London, 1964.

23. B. Miller, J. Electrochem. Soc. 116, 1675 (1969).

24. J. Ambrose, R.G. Barradas, D.W. Shoesmith, J. Electroanal. Chem. 47, 65 (1973).

25. V. Ashworth, D. Fairhurst, J. Electrochem. Soc. 124, 506 (1977).

26. S. Fletcher, R.G. Barradas, J.D. Porter, J. Electrochem. Soc. 125, 1960 (1978).

27. H.H. Strehblow and B. Titze, Electrochim. Acta 25, 839 (1980).

28. S.M. Abd, El Haleem and B.G. Ateya, J. Electroanal. Chem. 117, 309 (1981).

29. D.W. Shoesmith, S. Sunder, J.G. Bailey, G.J. Wallace and F.W. Stanchell, J. Electroanal. Chem. 143, 153 (1983).

30. G. Faita, G. Fiori and D. Salvadore, Corros. Sci. 15, 383 (1975).

31. W.D. Bjorndahl and Ken Nobe, Corrosion 40, 82 (1984).

32. M.H. Ghandehari, T.N. Andersen and H. Eyring, Corrosion Sci. 16, 123 (1976).

33. J. Venzcel, L. Knutsson and G. Wranglen, Corros. Sci. 4, 1 (1964).

34. C.H. Bonfiglio, J.C. Albaya and O.A. Cobo, Corros. Sci. 13, 717 (1973).

35. A.L. Bacarella and J.C. Griess, Jr., J. Electrochem. Soc. 120, 459 (1973).

36. W.D. Robertson, V.F. Nole, W.H. Davenport and F.P. Talboom, Jr., J. Electrochem. Soc. 105, 569 (1958).

37. P.J. King, "The Corrosion of Copper in Saline Environments", in Proceedings of a workshop on the Corrosion Performance of Nuclear Fuel Waste Containers, Atomic of Canada Limited, TR 340, 1983.

38. E.D. Mor and A.M. Beccaria, Corrosion 31, 275 (1975).

39. B.C. Syrett, Corrosion 33, 257 (1977).

40. H.S. Campbell, "A Review: Pitting Corrosion of Copper and Its Alloys", in Localized Corrosion, page 625-638, NACE, Houston, Texas, 1974.

41. D. Vasquez Moll, M.R.G. De Chialvo, R.C. Salvarezza and A.J. Arvia, Electrochim. Acta 30, 1011 (1985).

42. M. Romanoff, "Underground Corrosion", National Bureau of Standards Circular 579, 1957.

43. M. Pourbaix, J. van Muylder and P. van Laer, Corros. Sci. 7, 795 (1967).

44. I. Suzuki, Y. Ishikawa and Y. Hisamatsu, Corros. Sci. 23, 1095 (1983).

45. T. Fujii, T. Kodama and H. Baba, Corros. Sci. 24, 901 (1984).

46. M.R.G. De Chialvo, R.C. Salvarezza D. Vasquez Moll and A.J. Arvia, Electrochim. Acta 30, 1501 (1985).

47. M.G. Figueroa, R.C. Salvarezza and A.J. Arvia, Electrochim. Acta 31, 665 (1986).

48. E.Escalante and J. Kruger, J. Electrochem. Soc. 118, 1062 (1971).

49. L.A. Benjamin, D. Hardie and R.N. Parkins, Br. Corros. J. 23, 89 (1988).

50. Atomic Energy of Canada Limited, "Chemical Analysis of the Initial Groundwater Samples From the Lac Du Bonnet Batholith", Technical Record TR-21, 1979.

51. F. Mansfeld, Corrosion 29, 397 (1973).

52. R.L. LeRoy, Corrosion 31, 173 (1975).

53. F. King, C.D. Litke, K.W. Lam and P.J. King, "Corrosion of Copper", Atomic Energy of Canada Limited, TR-350, 1985.

54. W. Nernst, Z. Physik. Chem. 47, 52 (1904).

55. F.G. Cottrell, Z. Physik. Chem. 42, 385 (1902).

APPENDIX 1
ESTIMATION OF DIFFUSION CONTROLLED COPPER CORROSION RATE

Two mathematical approaches are used here to estimate copper corrosion depths controlled by a rate limiting diffusion reaction. In one approach, a constant concentration gradient is assumed and in the other, semi-infinite linear diffusion is supposed. Mathematical derivations using these assumptions have been generally used to describe various electrochemical systems, but most systems have a diffusion layer thickness of much less than a few millimeters and for a huge diffusion layer thickness as presumed here, the assumptions used in these approaches may not be valid. Nevertheless, these calculations may provide an estimate of the magnitude of copper corrosion as affected by diffusion.

A1-1.0 FIXED DIFFUSION LAYER

Assuming a fixed diffusion layer[54] with the diffusing species having a constant concentration at one end of the concentration gradient and a zero concentration at the other end, the limiting current for the half-reaction can be described by

$$i = n_L FADC/\delta$$

where n_L = number of electrons involved in the rate limiting half reaction
F = Faraday's constant
A = area of the electrode surface
D = diffusion coefficient
C = bulk concentration of the diffusing species
δ = fixed diffusion layer thickness

The charge over a time, t, for the constant limiting current is

$$Q_L = n_L FADCt/\delta$$

The charge consumed for the anodic oxidation of N moles of a material is governed by Faraday's law, which is expressed as

$$Q_a = n_a FN$$

where n_a = 1 for Cu/Cu^+.

For a corrosion reaction whose rate is controlled by a diffusion limited half reaction, the two charge expressions may be equated and rearranged to give

$$d = (n_L/n_a)(W/\rho)(D/\delta)Ct$$

where d = the corrosion depth
W = atomic weight of the material
ρ = density of the material

For corrosion of copper to the copper(I) state, the corrosion rate, R, in cm/a is

$$R = (2.247E8)n_L(D/\delta)C$$

where D is in cm^2/s, δ in cm and C in $moles/cm^3$.

The time, t_L, for establishing a diffusion layer of a certain thickness can be estimated from Einstein's equation,

$$\delta = (2Dt_L)^{1/2}$$

Arbitrarily assigning 25 cm as the thickness of the fixed diffusion layer and conservatively assigning 1×10^{-6} cm^2/s as the diffusion cofficient[7], the time required to establish a full concentration gradient across the layer is calculated to be 9.91 years.

Assuming

$D = 1 \times 10^{-6}$ cm^2/s and
C = 0.1 ppm,

if reduction of oxygen is rate limiting in the copper corrosion reaction, n_L is 4, and the corrosion rate, after 9.91 years, is estimated to be 1.12×10^{-3} µm/a.

If diffusion of copper(I) away from the corroding surface is rate determining, n_L is 1 and the corrosion rate is calculated to be 1.41×10^{-4} µm/a.

A1-2.0 SEMI-INFINITE LINEAR DIFFUSION

For a half reaction controlled by semi-infinite linear diffusion with the diffusing species having a zero concentration at one end of the concentration gradient, the current, i, can be described by the Cottrell equation[55] as,

$$i_d = n_dFAD^{1/2}C/(\pi t)^{1/2}$$

Integrating the equation over time gives

$$Q_d = 2n_dFAD^{1/2}Ct^{1/2}/\pi^{1/2}$$

Equating this diffusion controlled charge to the charge consumed in the anodic oxidation of the material as expressed by Faraday's law and rearranging gives a corrosion depth,

$$d = (2/\pi^{1/2})(n_d/n_a)(W/\rho)D^{1/2}Ct^{1/2}$$

Assuming

$D = 1 \times 10^{-6}$ cm^2/s and
C = 0.1 ppm,

and for a period of 9.91 years during which the diffusion layer would have grown to 25 cm, the depth

corroded from copper having a corrosion process controlled by oxygen diffusion is calculated to be 1.78 x 10^{-2} µm. If the corrosion process is controlled by the diffusion of copper(I) away from the corroding surface, the corrosion depth over 9.91 years is estimated to be 2.23 x 10^{-3} µm.

It must be emphasized that the diffusion controlled corrosion rate is directly proportional to the source concentration of the diffusing species. Here, the mathematical treatment regards the concentration as having a constant value, which during the early stages of the operation of the disposal vault may vary considerably. For example, oxygen trapped during vault closure will greatly increase its concentration in groundwater. Also other processes, such as adsorption and ion exchange on the buffer material, may distort the concentration profiles in the diffusion layer and thus, may affect the corrosion rate.

APPENDIX 2

PREPARATION OF WN1 SALINE GROUNDWATER

The original procedure for the preparation of the WN1 solution was supplied by Atomic Energy of Canada Limited. The following is a version modified by Ontario Hydro's Analytical Services Section. The recipe provides 10L of WN1 solution.

1. Prepare a 1L stock solution with the following chemicals:

conc. HC1	1.0 mL
KC1	2.686g
$NaNO_3$	4.505g
$SrC1_2.6H_2O$	7.400g
$FeSO_4.7H_2O$	0.278g

2. Prepare 10L of WN1 solution by using,

stock solution	100mL
conc. H_2SO_4	4.7mL
$CaC1_2.2H_2O$	65.556g
NaC1	47.602g
$MgSO_4.7H_2O$	6.126g
$NaHCO_3$	0.941g
$Ca(OH)_2$	6.409g

Allow the solution to stand for a day and adjust the solution pH to ~7.0 with 1:10 HC1. Filter the solution with #40 Whatman paper and, before use, with 0.45µm millipore filter paper.

APPENDIX 3

RADIOLYSIS TEST RIG

A3-1.0 LOCATION

The experiments to study the effects of radiation on the corrosion of copper were performed in the Auxiliary Irradiated Fuel Bay (AIFB) of Pickering Nuclear Generating Station. The south side of the bay, which had minimal interference from station activity, was chosen as the location to conduct the study. Corrosion coupons immersed in the test medium were contained in autoclaves. A steel cylinder enclosing the autoclaves was placed on the bay floor below 7.3 m of water in the 45 cm gap between the bay wall and the stacks of baskets of irradiated fuel bundles (Figure A3-1). The irradiated fuel bundles beside the steel cylinder were 7 years old at the start of the study. Radiation rate measurement taken at the end of the study read ~1000 Rad/h at the fuel bundles, ~70 Rad/h at the wall, and ~150 Rad/h within the container.

A3-2.0 CYLINDER CONTAINER

Figure A3-2 shows a cross section of the water tight container. The body of the container was fabricated from a sheet of AISI 316 stainless steel by rolling the sheet into a cylinder and welding its edges together. After the bottom plate and top flange were welded onto the body, the container was heat treated at ~1100°C and water quenched. The thickness of the container wall was 3.175 mm. The bottom plate, top flange and top cover plate were each 6.35 mm thick. The internal diameter of the container was 23.5 cm and the internal length was 92.1 cm. The top cover plate was fastened to the flange by a set of twelve nuts and bolts. It had lugs for suspending the container and also Conax fittings with viton seal for power and signal wires to pass through (Figures A3-3 and A3-4). Barrier terminal blocks, Coaxicon contacts and thermocouple plugs positioned under the top cover plate for wire connection allowed unrestricted removal of the header away from the container when it was necessary.

Sealing between the header and the top flange was by a 3.175 mm thick silicone rubber gasket. Water tightness was ensured by application of acrylic base sealants (Loctite) to all threaded parts and by sealing the Conax fitting with epoxy. Before commissioning, the entire assembly was tested for leaks in a water tank pressurized at 172.4 kPa, which was greater than twice the external pressure exerted on the container at the bottom of the bay.

A3-3.0 AUTOCLAVE

The container was designed to accommodate a vertical rack of three autoclaves. The rack had three removable stainless steel shelves. Each contained an autoclave unit, supported by three stainless steel rods and fastened to the next shelf by nuts at the threaded ends of the support rods. A 2.54 mm thick alumina-silica insulation plate separated the rack from the wire connectors at the top of the container.

Figure A3-5 shows a cross section of an autoclave unit. The autoclave was made of Inconel 600, a Ni-Cr-Fe alloy. Its wall thickness was 3.175 mm and its top flange and cover plate were 6.35 mm thick. Its internal dimensions were 8.3 cm in diameter and 15.9 cm in height. A 2 mm thick glass vessel lined its internal wall. Closure of the cover plate was by nuts and bolts, and sealing of the closure was by a silicone rubber 0-ring seated in a groove on the flange. Conax fittings with viton seals on the cover plate allowed passage of a gas purge line, a thermocouple and electrode leads into the vessel. The electrode lead was insulated within the vessel by a glass tubing. Viton seals and silicone rubber gaskets sealed the glass tubing at both ends. A 200 W band heater supplied heat to the autoclave and a 2.54 cm thick calcium

silicate autoclave shell provided insulation. Thermal tests at an autoclave operating temperature of 150°C recorded a temperature of 35°C in the top section of the cylinder container and up to 50°C at the outer wall of the autoclave insulation. The autoclave was pressure tested with saturated steam pressure at 200°C before commissioning.

A3-4.0 INSTRUMENTATION

Figure A3-6 shows a block diagram of the electric circuit of the experiment. In each power supplying circuit, a ground fault detector protected the system from short circuiting. A temperature controller coupled with a variable transformer controlled the temperature of each autoclave. A two channel high temperature limit controller guarded the system from run away temperature.

The electrochemical system (Figure A3-7) was consisted of a potentiostat with a sweep generator. A digital voltmeter measured current as IR drop across a resistor in the negative feedback loop of the potentiostat, and a X-Y recorder recorded current-potential data.

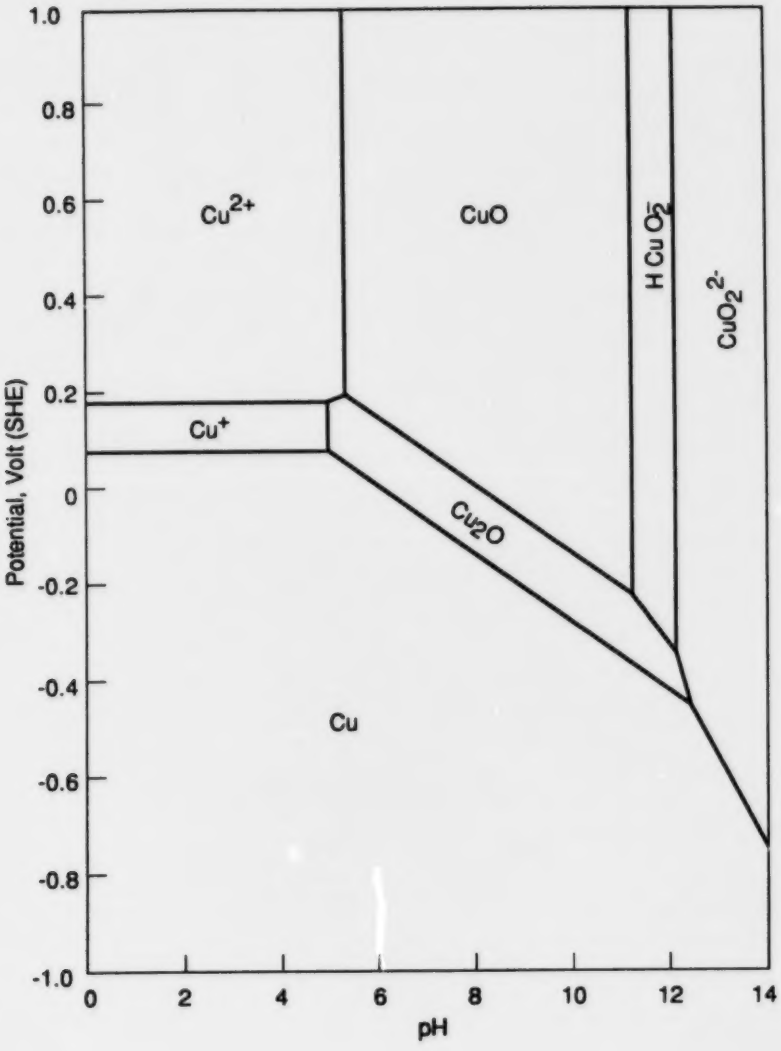

FIGURE 3-1

POTENTIAL-pH DIAGRAM FOR Cu-H_2O AT 100C; 1μ M IONIC COPPER

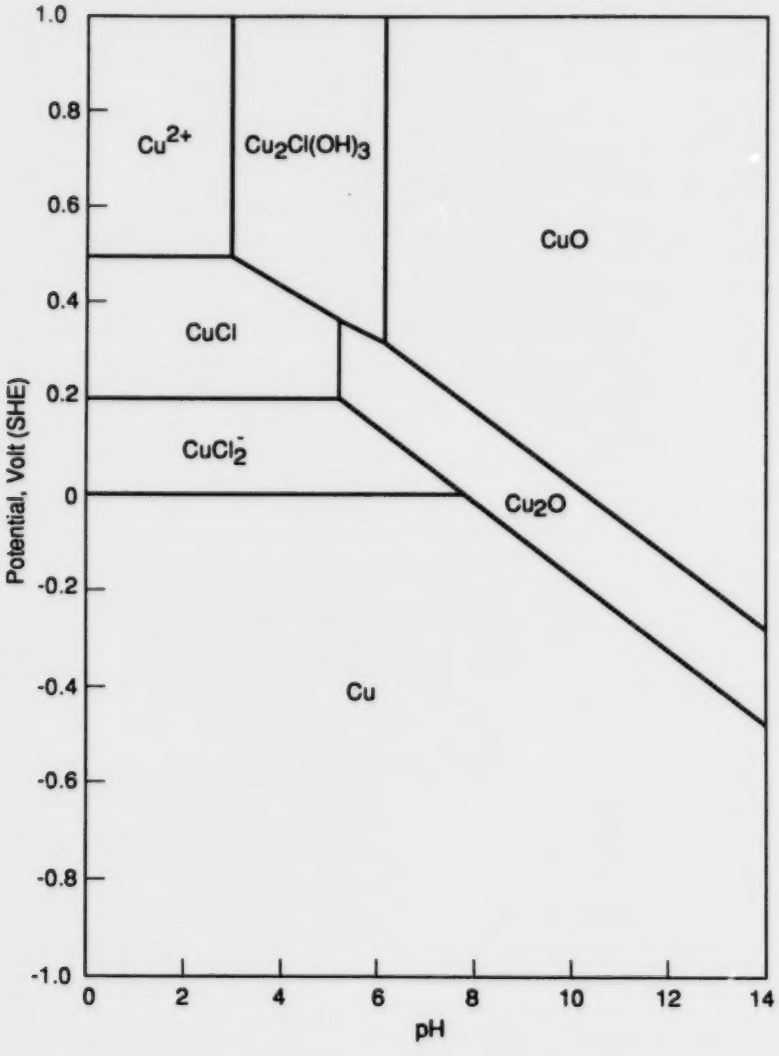

FIGURE 3.2

POTENTIAL-pH DIAGRAM FOR Cu-Cl-H2O AT 25C; 0.1 M CHLORIDE, 1μM IONIC COPPER

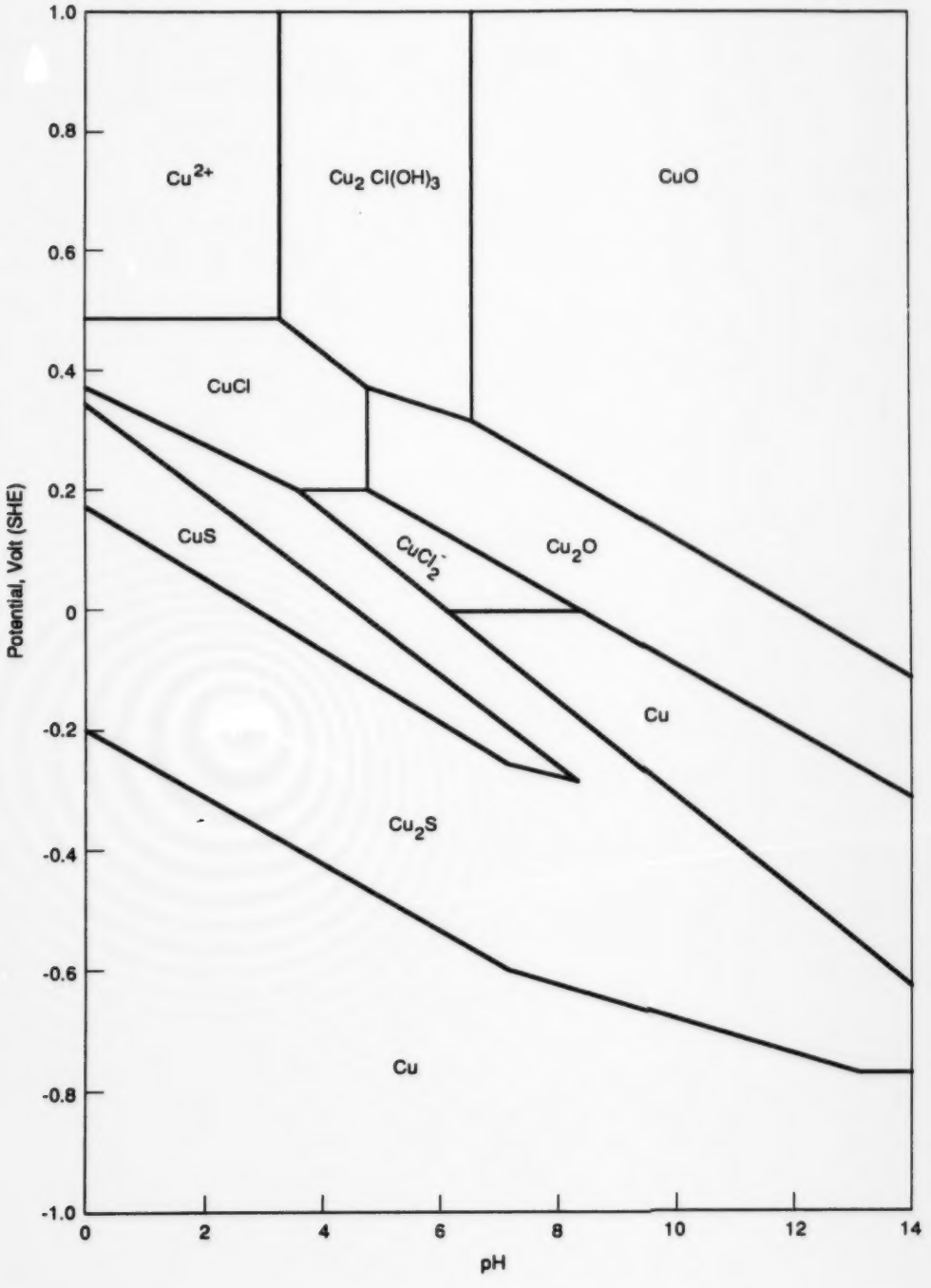

FIGURE 3.3

POTENTIAL - pH DIAGRAM FOR Cu-Cl-S-H_2O AT 25°C; 0.1 M CHLORIDE, 0.1 mM SULPHIDE, 1 μM IONIC COPPER

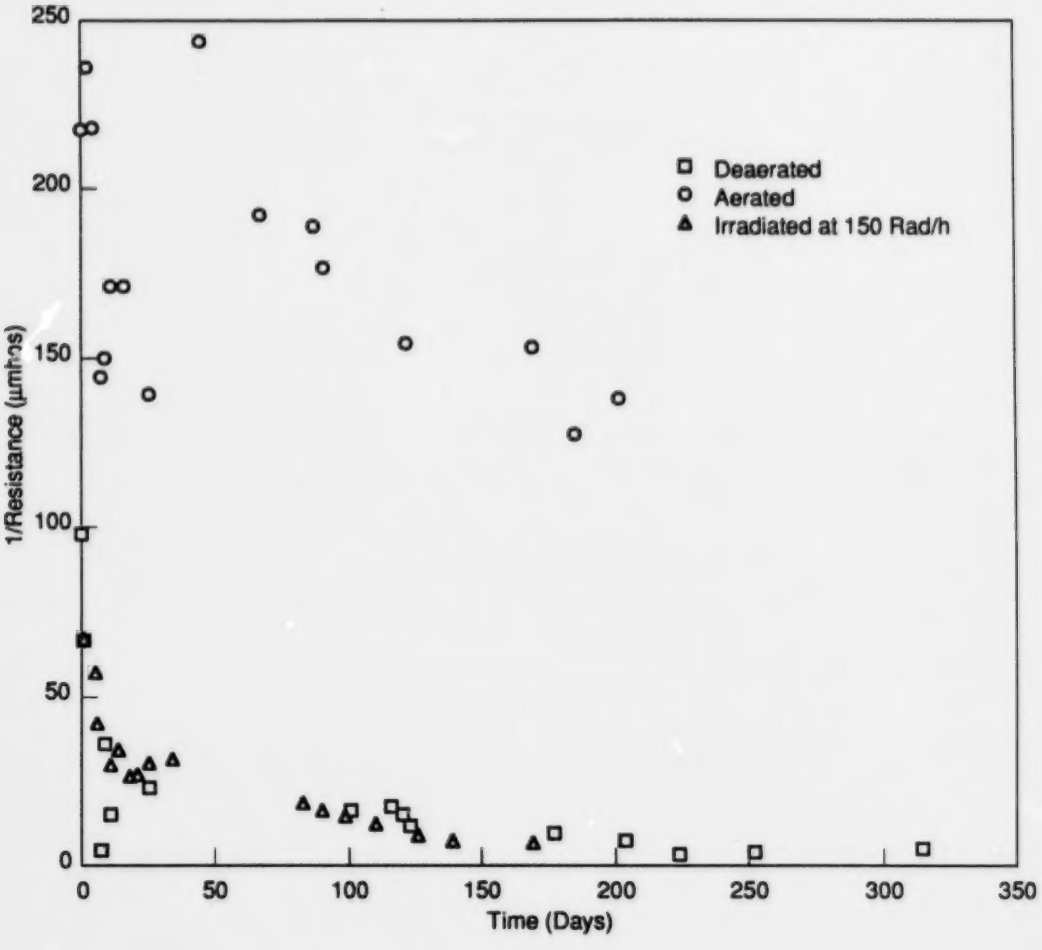

FIGURE 5-1

CORROSION RATE-TIME TREND OF COPPER IN A SYNTHETIC WNI GROUNDWATER - BENTONITE SLURRY (4 mL: 1 g) AT 75C

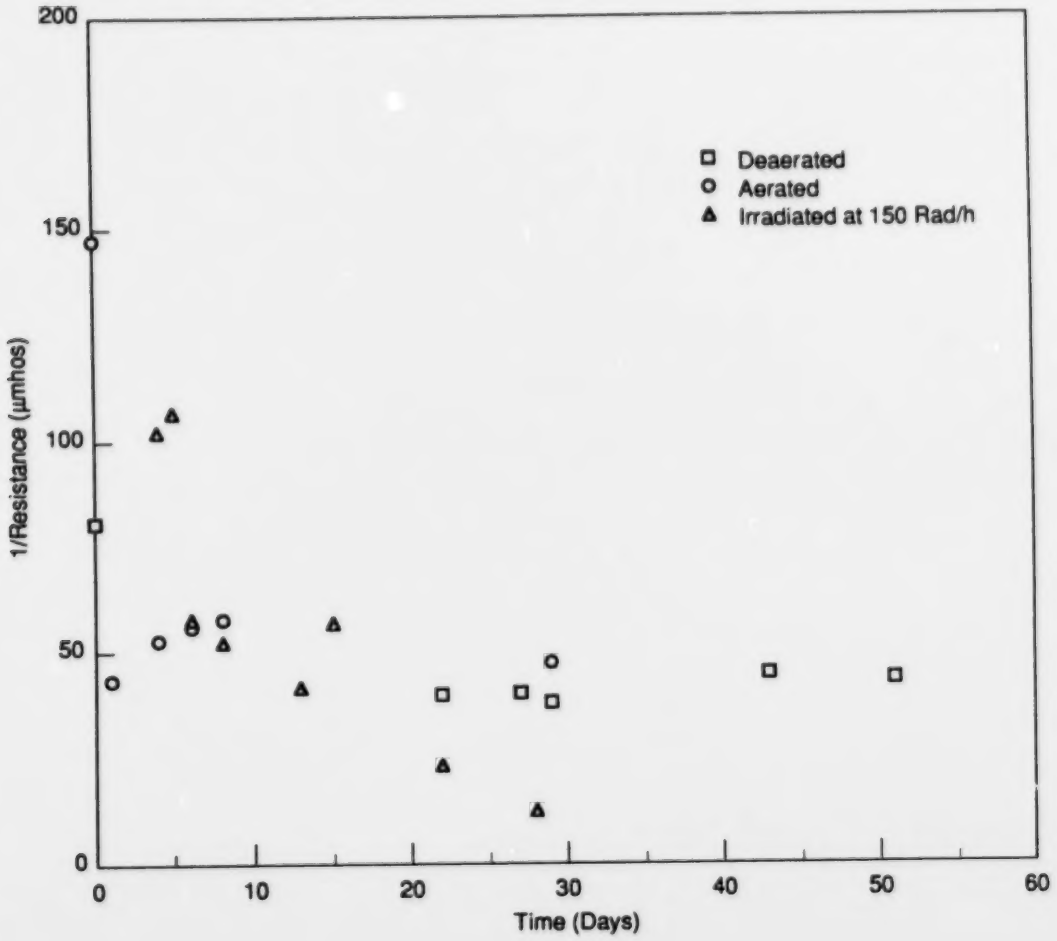

FIGURE 5-2

CORROSION RATE-TIME TREND OF COPPER IN A SYNTHETIC WNI GROUNDWATER - BENTONITE SLURRY (4 mL: 1 g) AT 150C

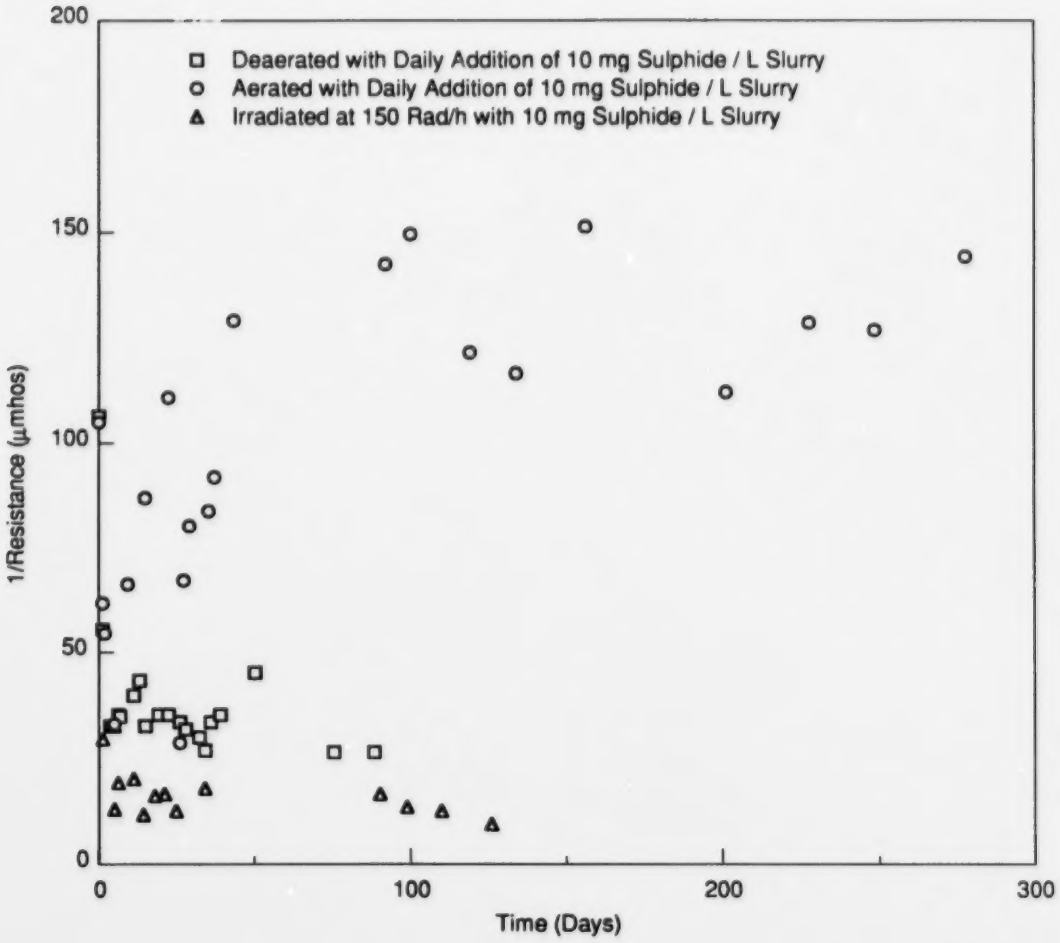

FIGURE 5-3

CORROSION RATE-TIME TREND OF COPPER IN A SYNTHETIC WNI GROUNDWATER - BENTONITE SLURRY (4 mL: 1 g) AT 75C

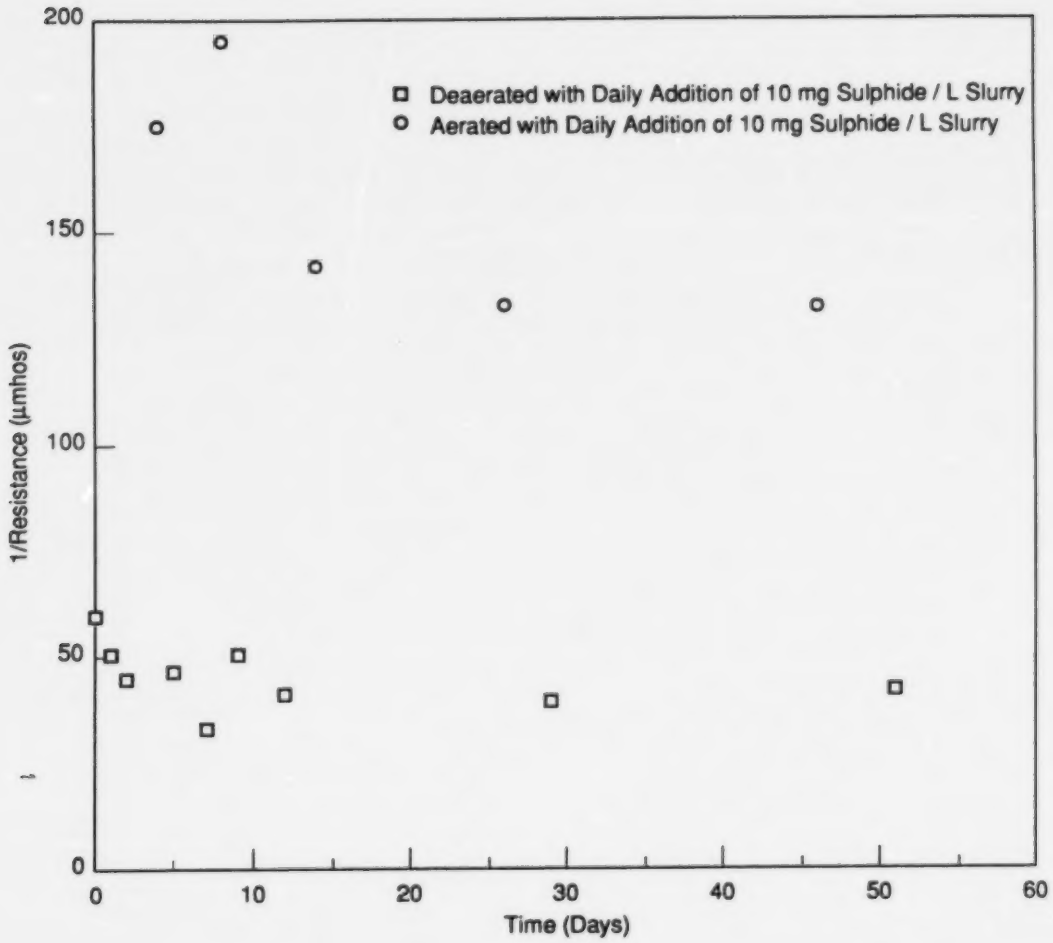

FIGURE 5-4

CORROSION RATE-TIME TREND OF COPPER IN A SYNTHETIC WNI GROUNDWATER - BENTONITE SLURRY (4 mL: 1 g) AT 150C

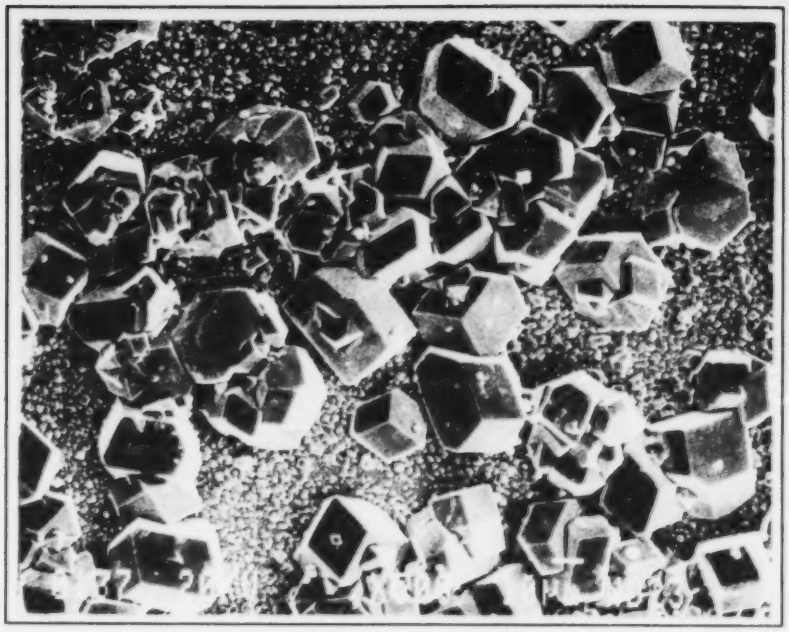

20μm

(a) WITHOUT SULPHIDE;
SHOWING CUBIC/OCTAHEDRAL CRYSTALS OF CUPROUS OXIDE

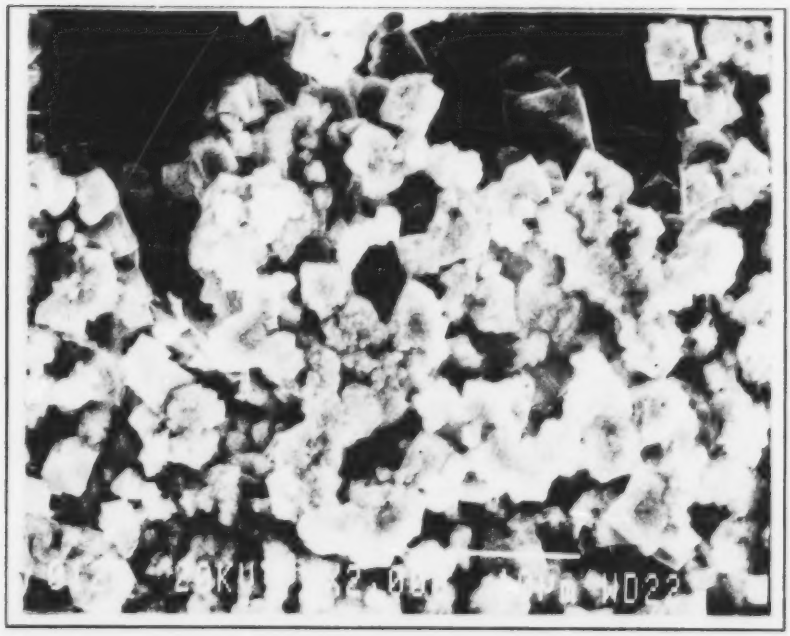

5μm

(b) WITH 10 mg/L OF SULPHIDES;
SHOWING A PATCH OF ORTHORHOMBIC COPPER CHLORIDE HYDROXIDE

FIGURE 5-5

CORROSION PRODUCT OF COPPER AFTER IRRADIATION AT 150 RAD/h FOR 262 DAYS AT 75C IN A WN1 GROUNDWATER-BENTONITE SLURRY (4 mL: 1 g)

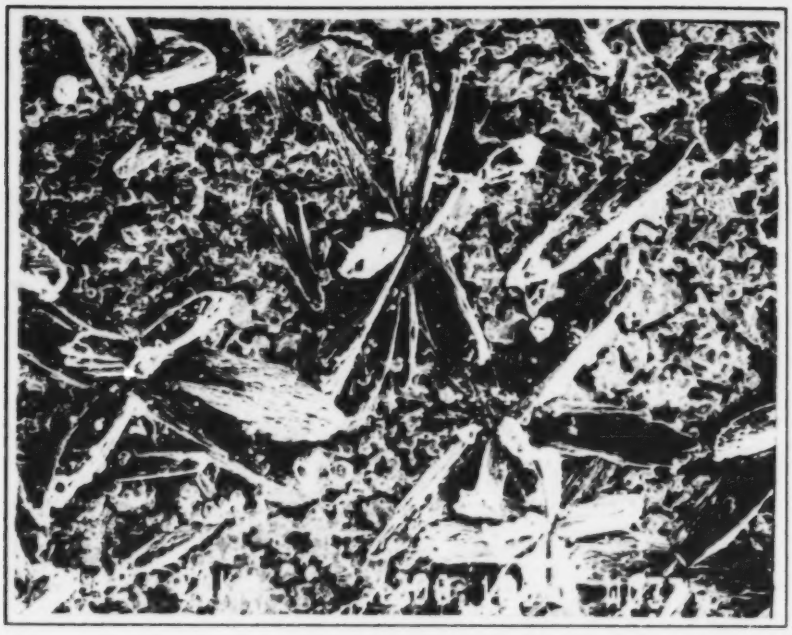

50μ m

(a) SHOWING CALCIUM CARBONATE (STAR SHAPED) DEPOSITED ON A PATCH OF POROUS CUPROUS OXIDE

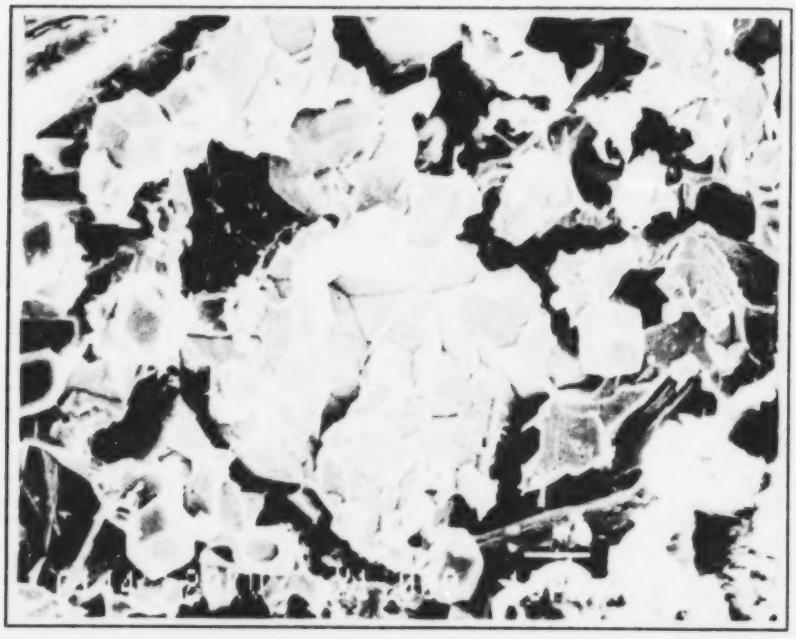

10μ m

(b) SHOWING A POROUS LAYER OF CUBIC CUPROUS OXIDE

FIGURE 5-6

CORROSION PRODUCT OF COPPER AFTER IRRADIATION AT 150 RAD/h FOR 150 DAYS AT 150C IN A WN1 GROUNDWATER-BENTONITE SLURRY (4 mL: 1 g)

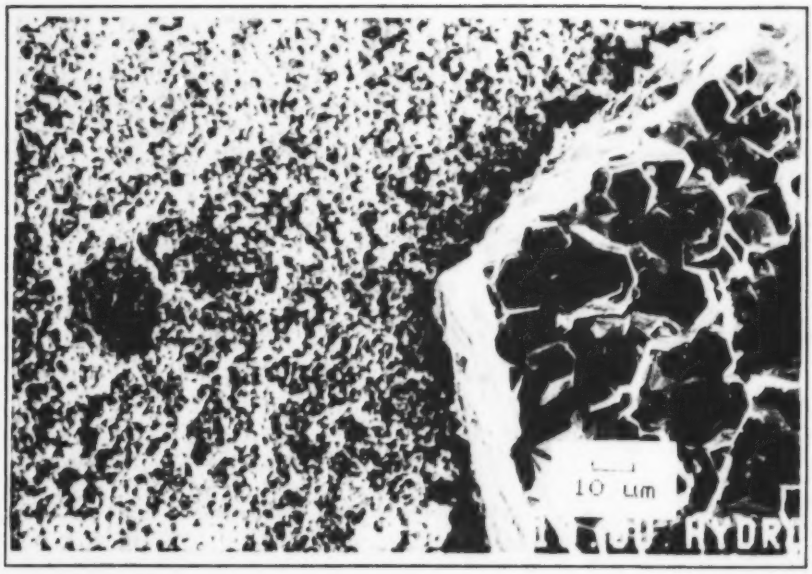

FIGURE 5-7

DUAL LAYER OF CUPROUS SULPHIDE. PART OF THE TOP LAYER WAS PEELED OFF TO REVEAL THE BOTTOM LAYER. THE COPPER COUPON HAS BEEN EXPOSED IN A WN1 GROUNDWATER-BENTONITE SLURRY (4 mL: 1g) CONTAINING SULPHIDE AT 75C FOR ~1 YEAR

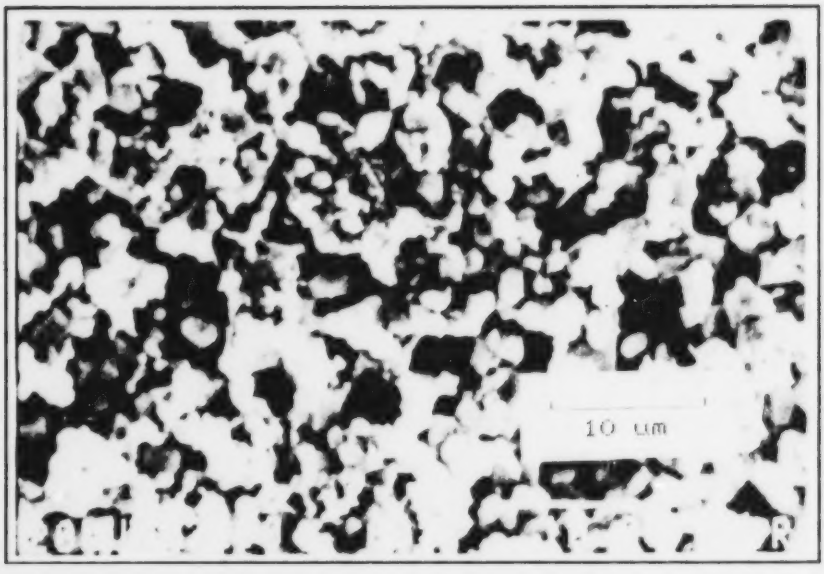

FIGURE 5-8

THE INNER LAYER OF A DUAL LAYER OF CUPROUS SULPHIDE SHOWING A POROUS STRUCTURE

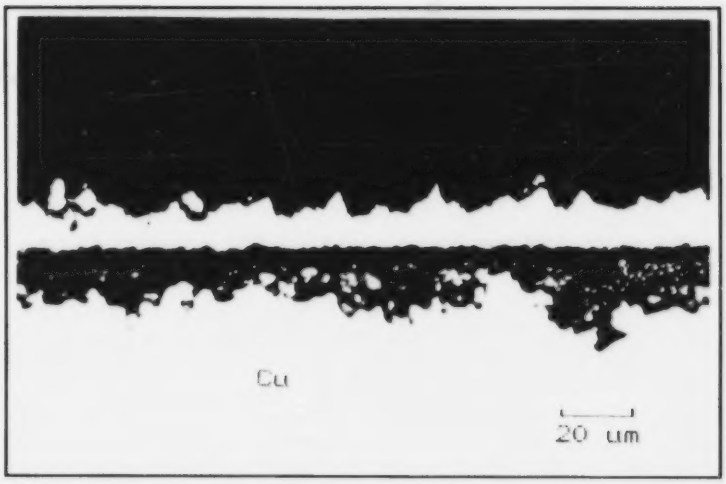

FIGURE 5-9

CROSS SECTION OF A COPPER COUPON SHOWING A DUAL LAYER OF CUPROUS SULPHIDE WITH THE INNER LAYER FIRMLY ADHERED ON COPPER'S CORRODED SURFACE

(a) FOR 186 DAYS

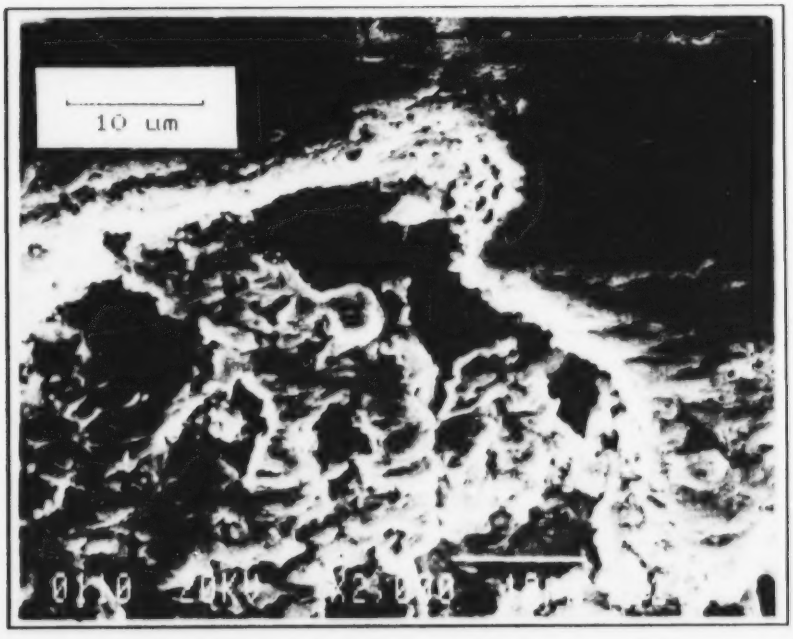

(b) WITH SULPHIDE FOR 127 DAYS

FIGURE 5-10

PITTING AND ROUGHENED SURFACE OF COPPER AFTER EXPOSURE AT 75C IN A DEAERATED WN1 GROUNDWATER-BENTONITE SLURRY

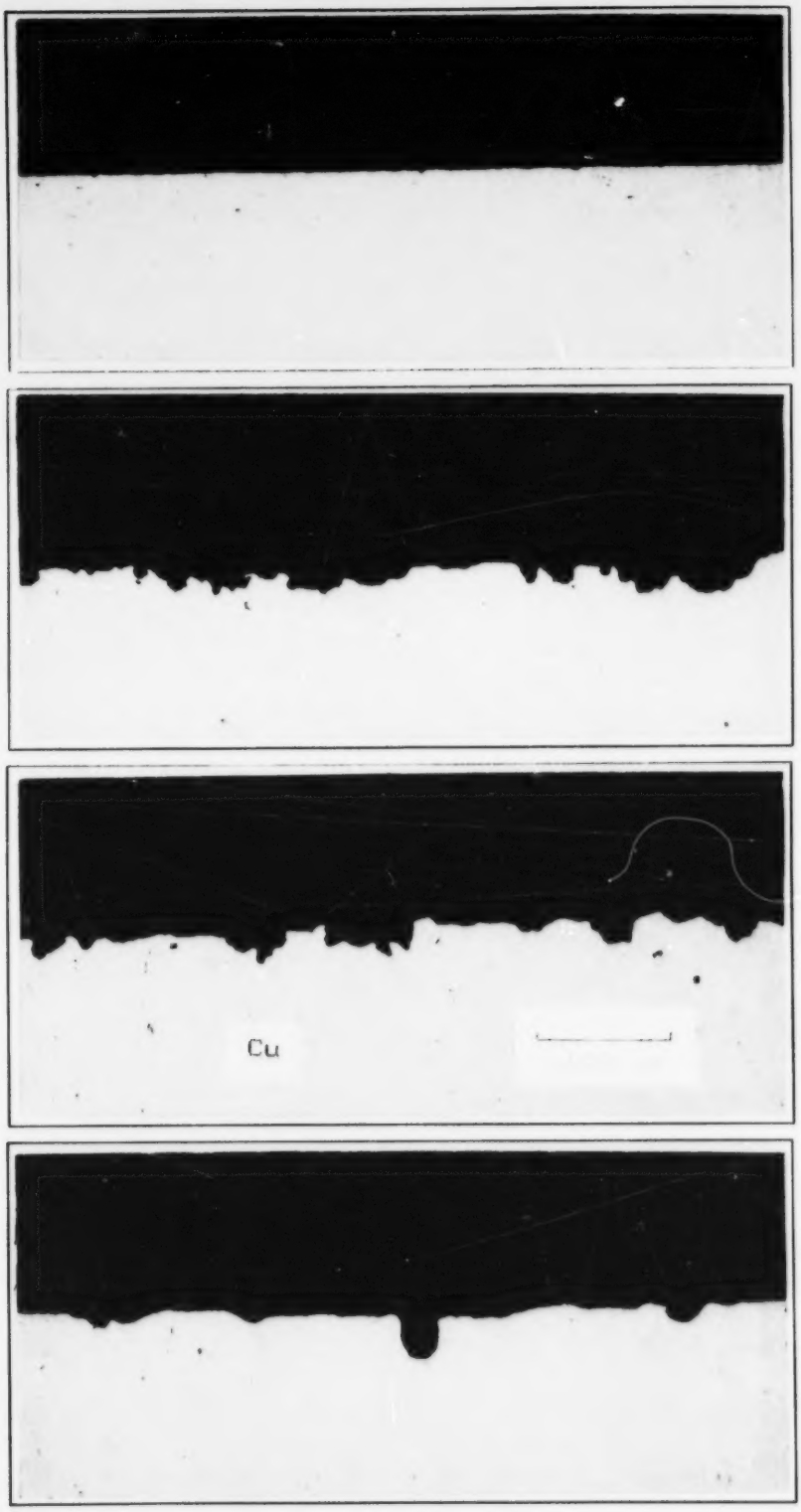

FIGURE 5-11

CROSS SECTION OF PITS ON COPPER AFTER EXPOSURE AT 75C IN A WN1 GROUNDWATER-BENTONITE SLURRY

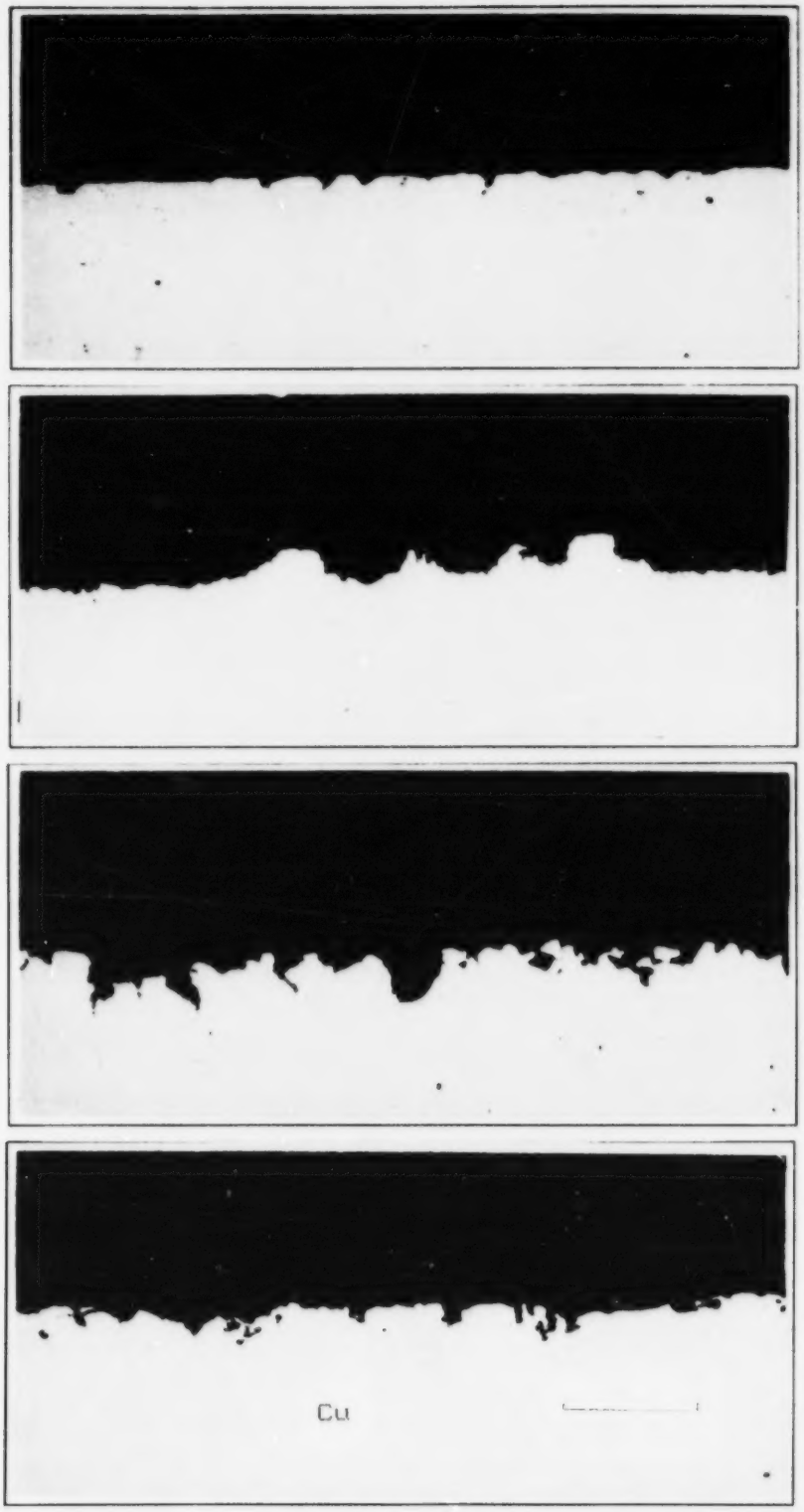

FIGURE 5-12

CROSS SECTION OF PITS ON COPPER AFTER EXPOSURE AT 150C IN A WN1 GROUNDWATER-BENTONITE SLURRY

180796-L7-RD

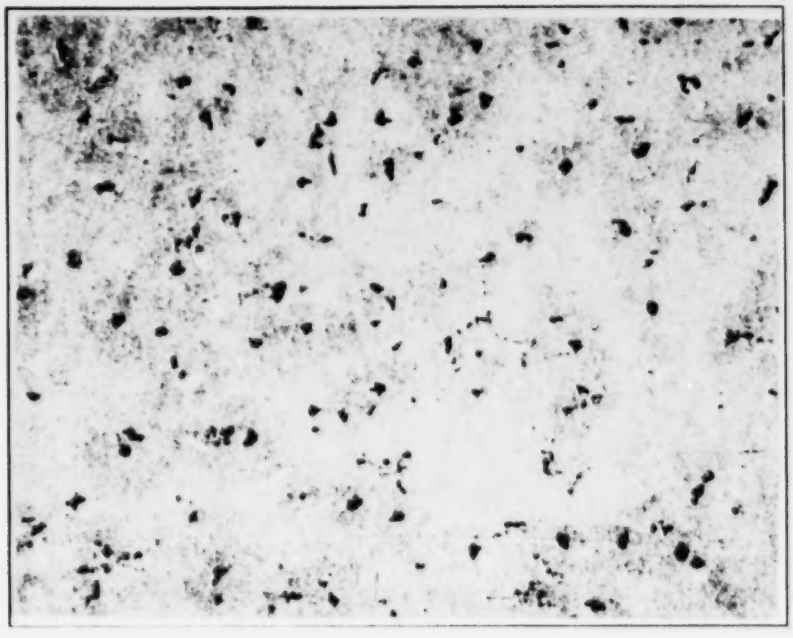

0.1 mm

(a) AT 75C FOR 262 DAYS

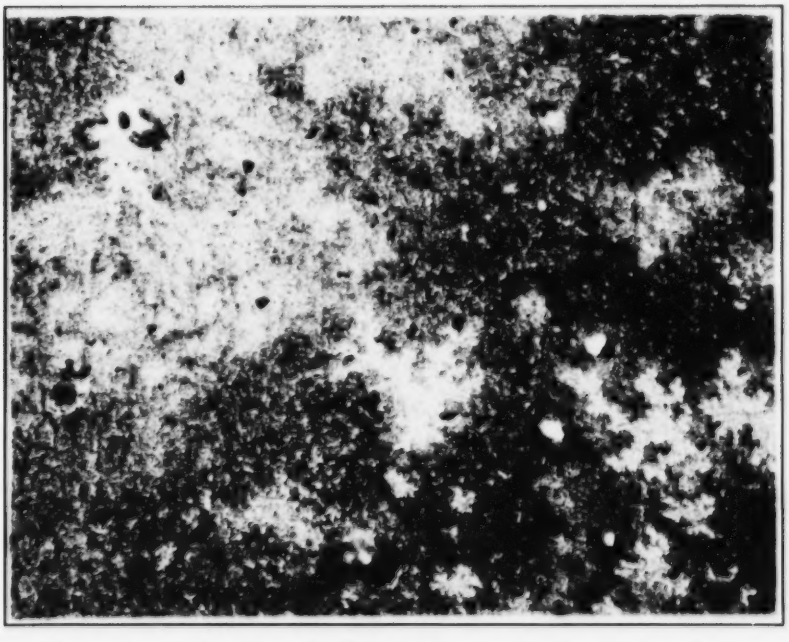

0.1 mm

(b) WITH 10 mg/L OF SULPHIDE AT 150C FOR 150 DAYS

FIGURE 5-13

PITTING THROUGH CORROSION PRODUCT ON A COPPER COUPON AFTER IRRADIATION AT 150 RAD/h IN A DEAERATED WN1 GROUNDWATER-BENTONITE SLURRY (4 mL: 1 g)

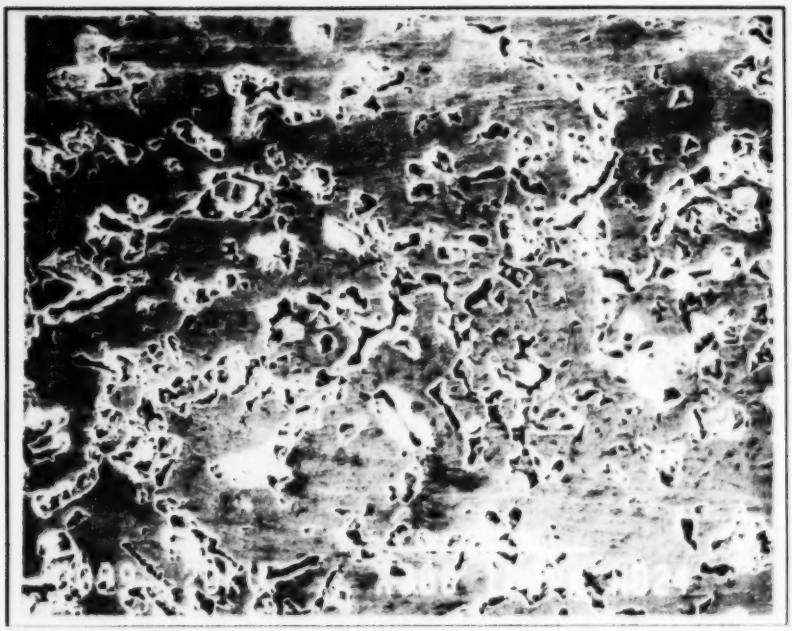

33μm

(a) WITH 10 mg/L OF SULPHIDE

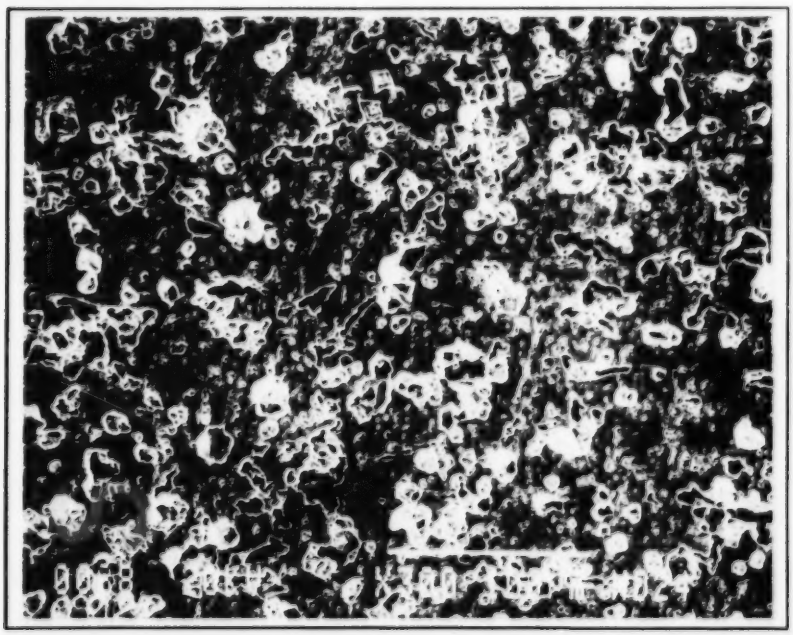

33μm

(b) WITHOUT SULPHIDE

FIGURE 5-14

HIGH DENSITY OF IRREGULARLY SHAPED PITS OF VARIOUS SIZES ON COPPER AFTER IRRADIATION AT 150 RAD/h IN A DEAERATED WN1 GROUNDWATER-BENTONITE SLURRY (4 mg: 1g) at 75C FOR 262 DAYS

180798-L7-RD

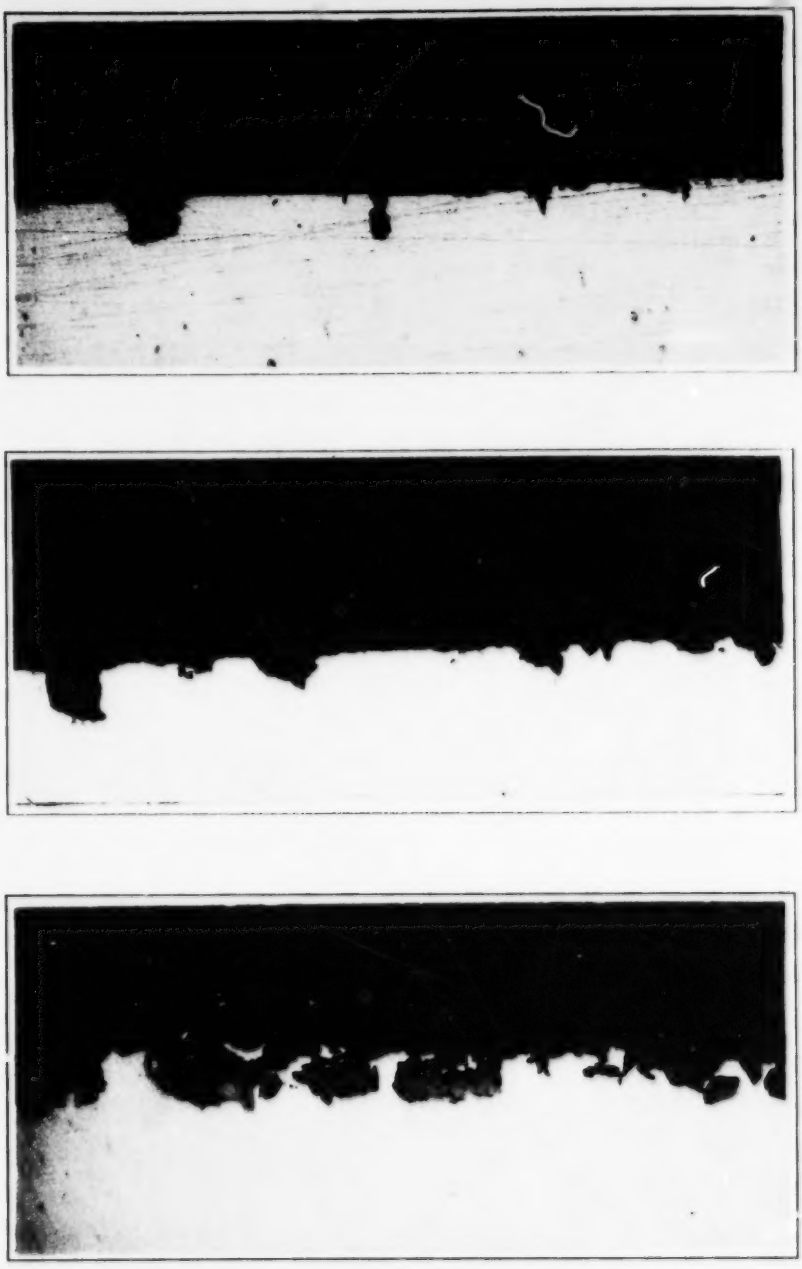

(a)
AT 75C:
FOR 262 DAYS

50 µm

(b)
WITH 10 mg/L OF
SULPHIDE AT 75C
FOR 262 DAYS

50 µm

(c)
AT 150C FOR 150 DAYS
SHOWING CORROSION
PRODUCT WITHIN PITS

100 µm

FIGURE 5-15

CROSS SECTION OF COPPER AFTER IRRADIATION AT 150 RAD/h IN A DEAERATED WN1 GROUNDWATER-BENTONITE SLURRY

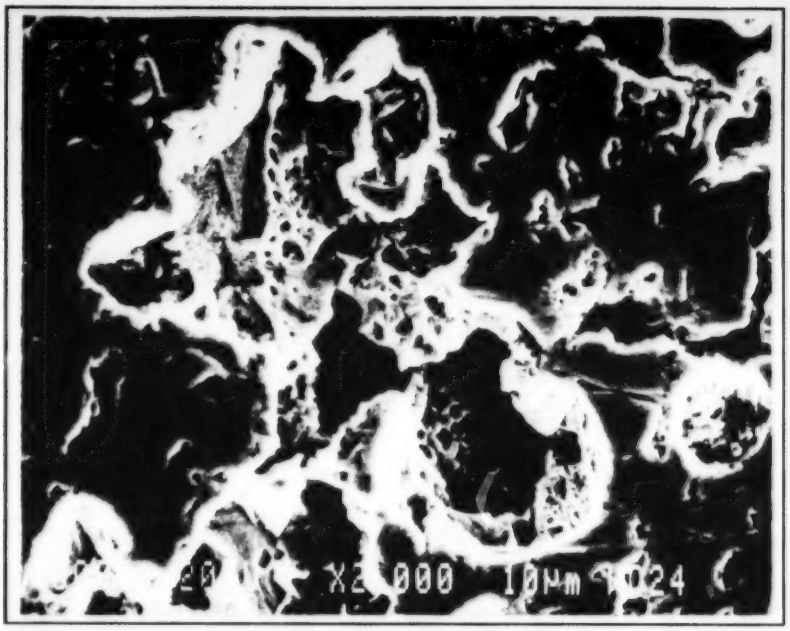

(a) AT 75C FOR 262 DAYS SHOWING MICROPITS AND CRYSTALLOGRAPHIC PLANES WITHIN PITS

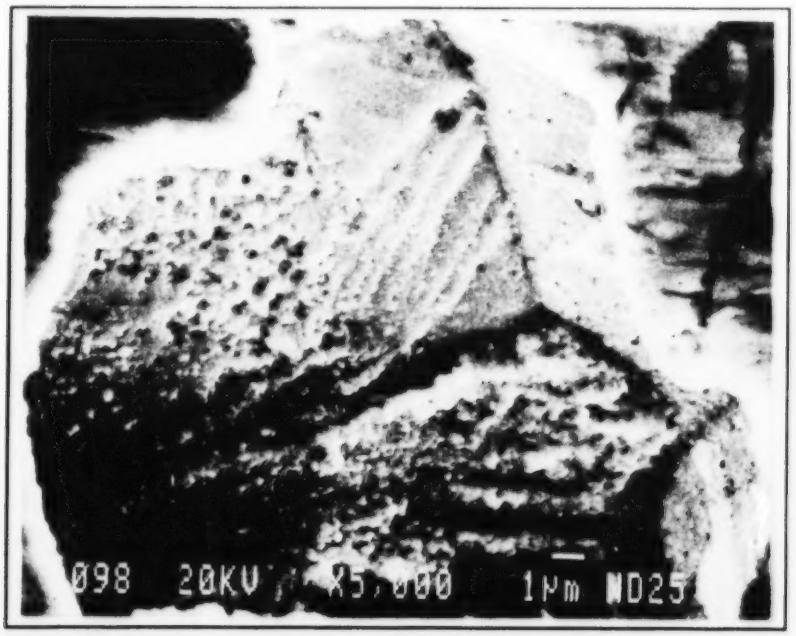

(b) WITH 10 mg/L OF SULPHIDE AT 150C FOR 150 DAYS SHOWING CRYSTALLOGRAPHIC PLANES WITHIN PITS

FIGURE 5-16

PITS ON COPPER AFTER IRRADIATION AT 150 RAD/h IN A DEAERATED WN1 GROUNDWATER-BENTONITE SLURRY (4mL: 1g)

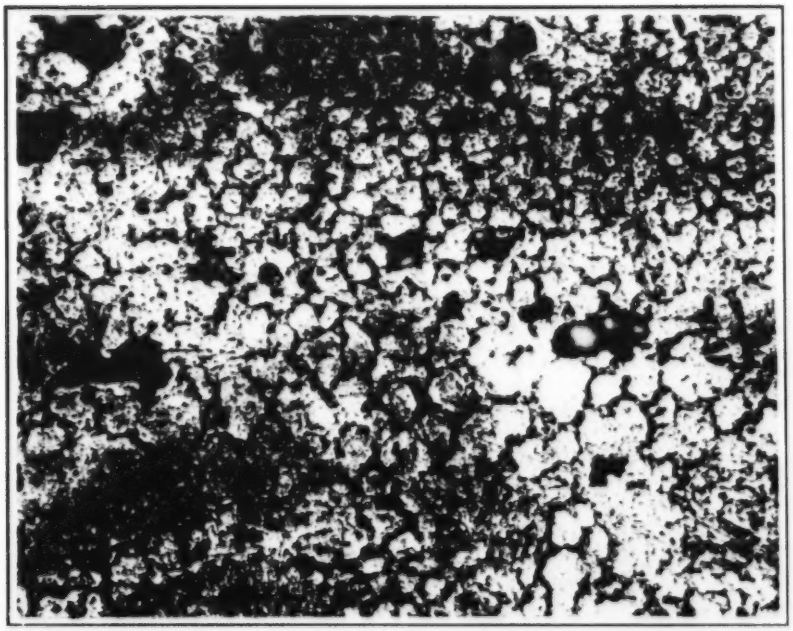

FIGURE 5-17

INTERGRANULAR ATTACK ON COPPER AFTER IRRADIATION AT 150 RAD/h IN A DEAERATED WN1 GROUNDWATER-BENTONITE SLURRY (4 mL: 1g) WITH 10 mg/L OF SULPHIDE AT 150C FOR 150 DAYS

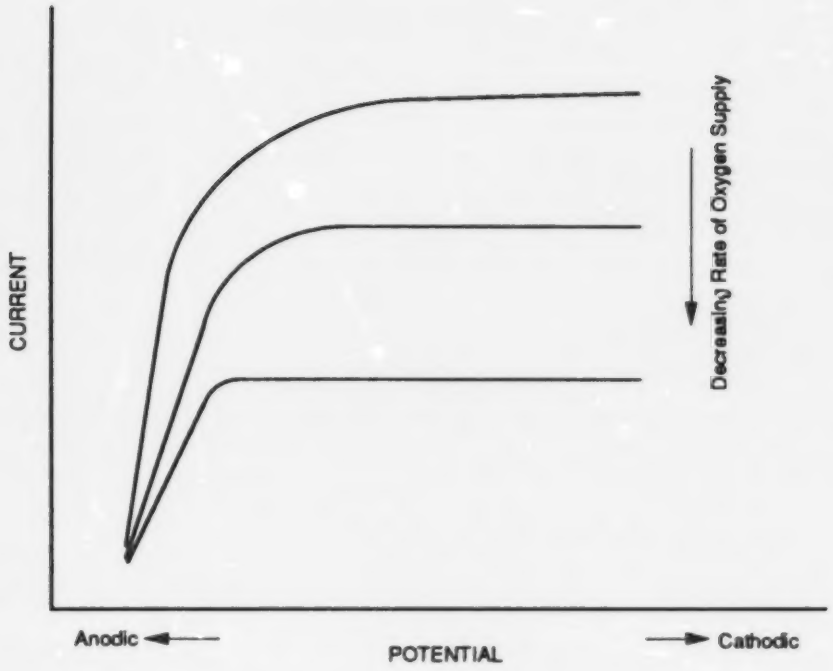

FIGURE 6-1

CURRENT-POTENTIAL CURVES OF OXYGEN REDUCTION ON COPPER IN A SALINE SOLUTION ILLUSTRATING THE ANODIC SHIFT IN THE POTENTIAL OF THE LIMITING CURRENT WITH A DECREASEING RATE OF SUPPLY OF OXYGEN
(Adapted from Reference 33)

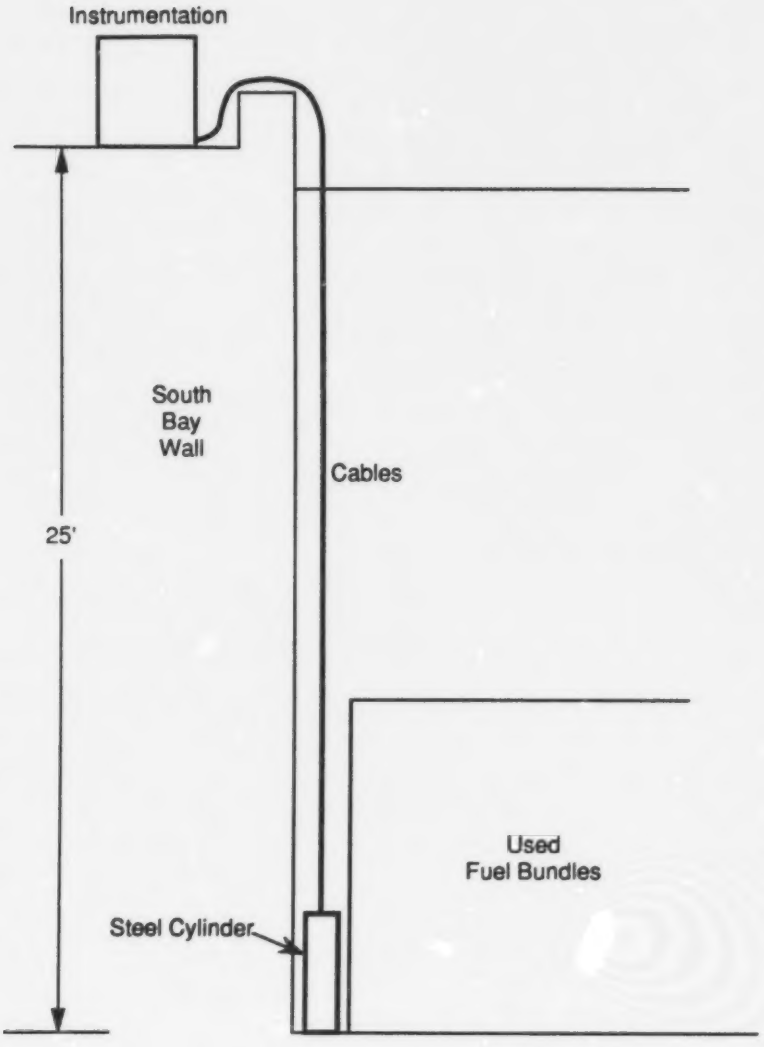

FIGURE A3-1

**LOCATION OF RADIOLYSIS EXPERIMENT
IN PNGS AUXILIARY IRRADIATED FUEL BAY**

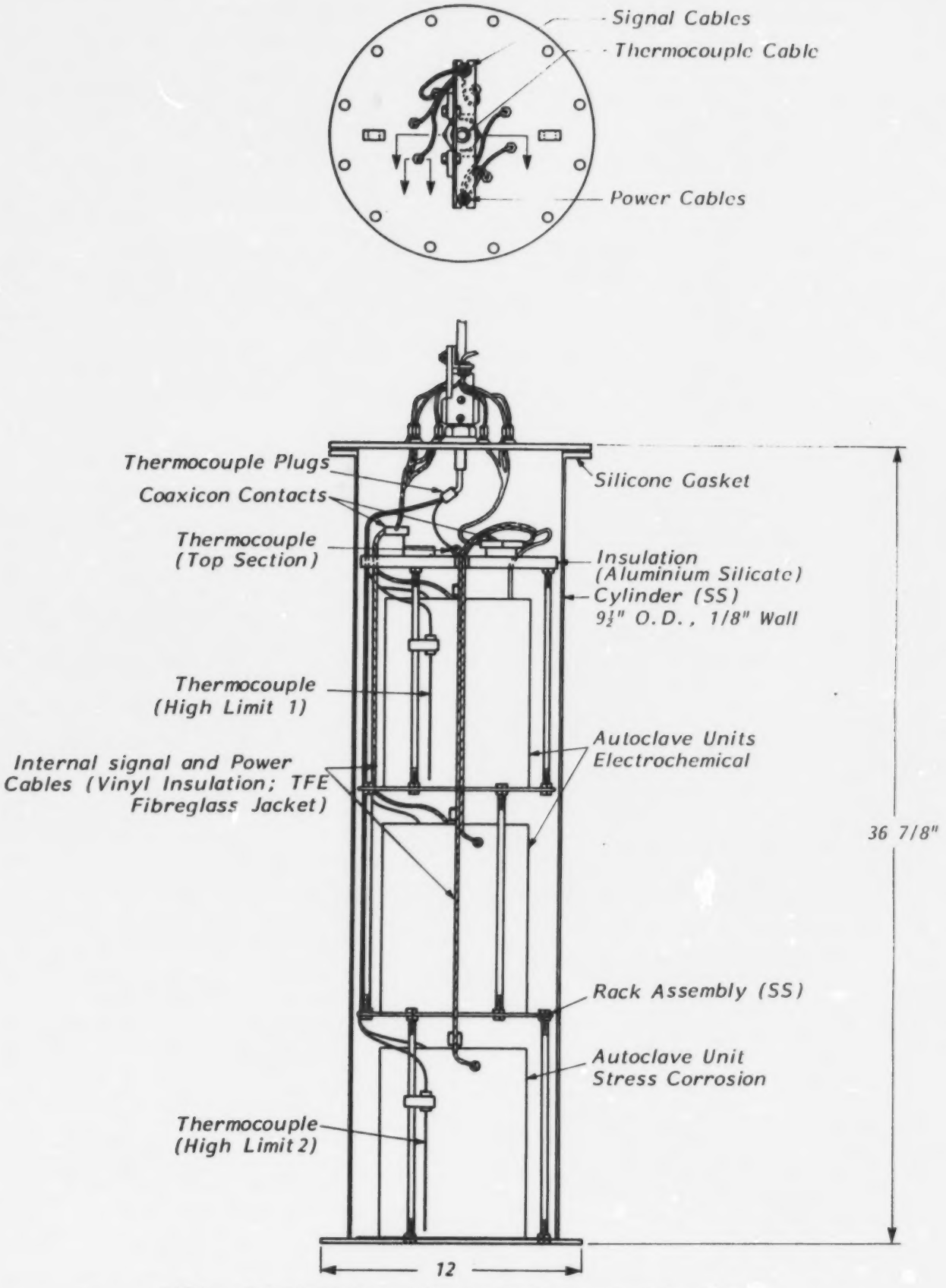

Lifting Attachments and Heater Bolts Removed for Clarity

FIGURE A3-2

CROSS SECTION OF WATER TIGHT CYLINDER FOR RADIOLYSIS EXPERIMENTS

169458-RD

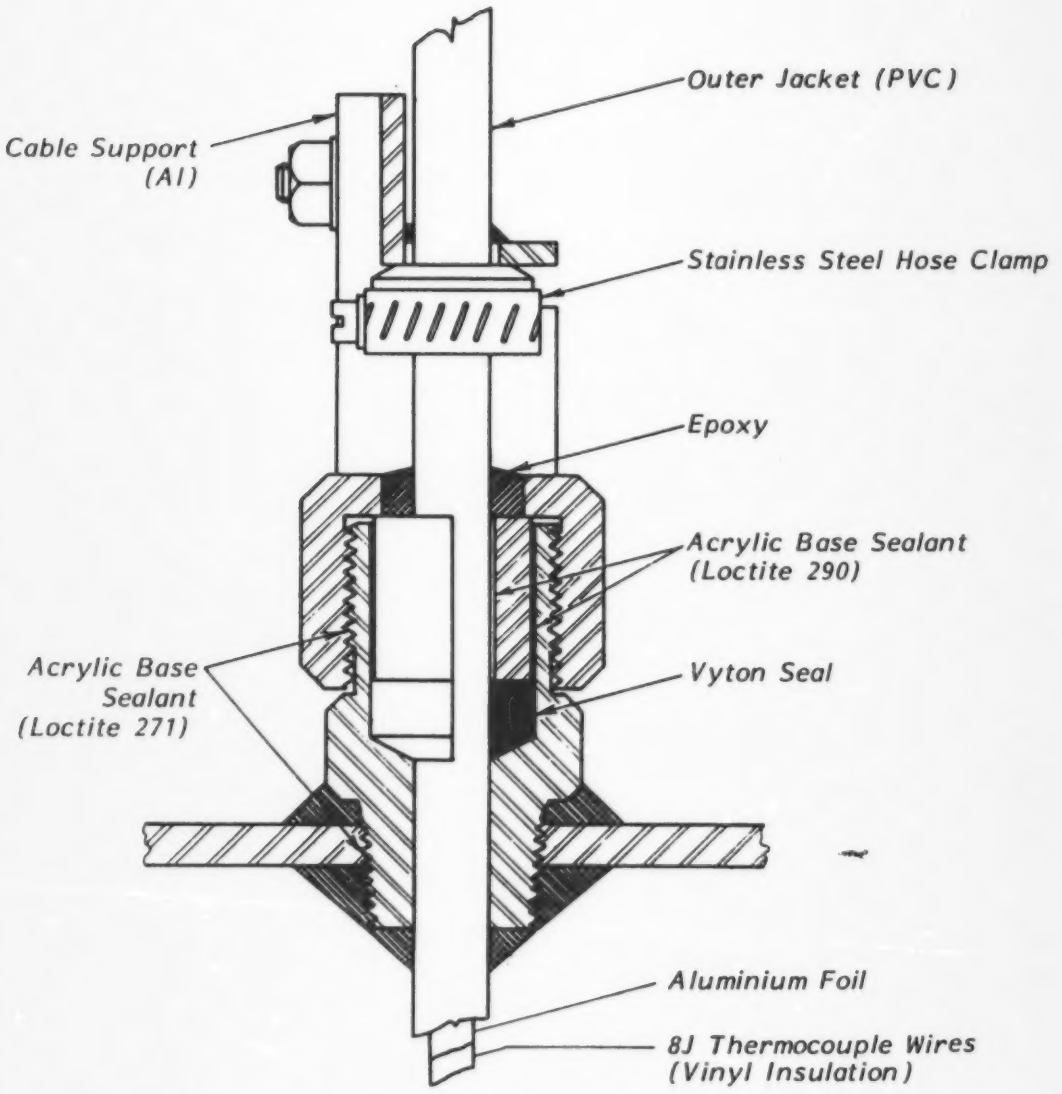

FIGURE A3-3

CROSS SECTION OF AA CONAX PG5 - 500 - A-V FITTING AND CABLE SUPPORT ON CYLINDER COVER PLATE

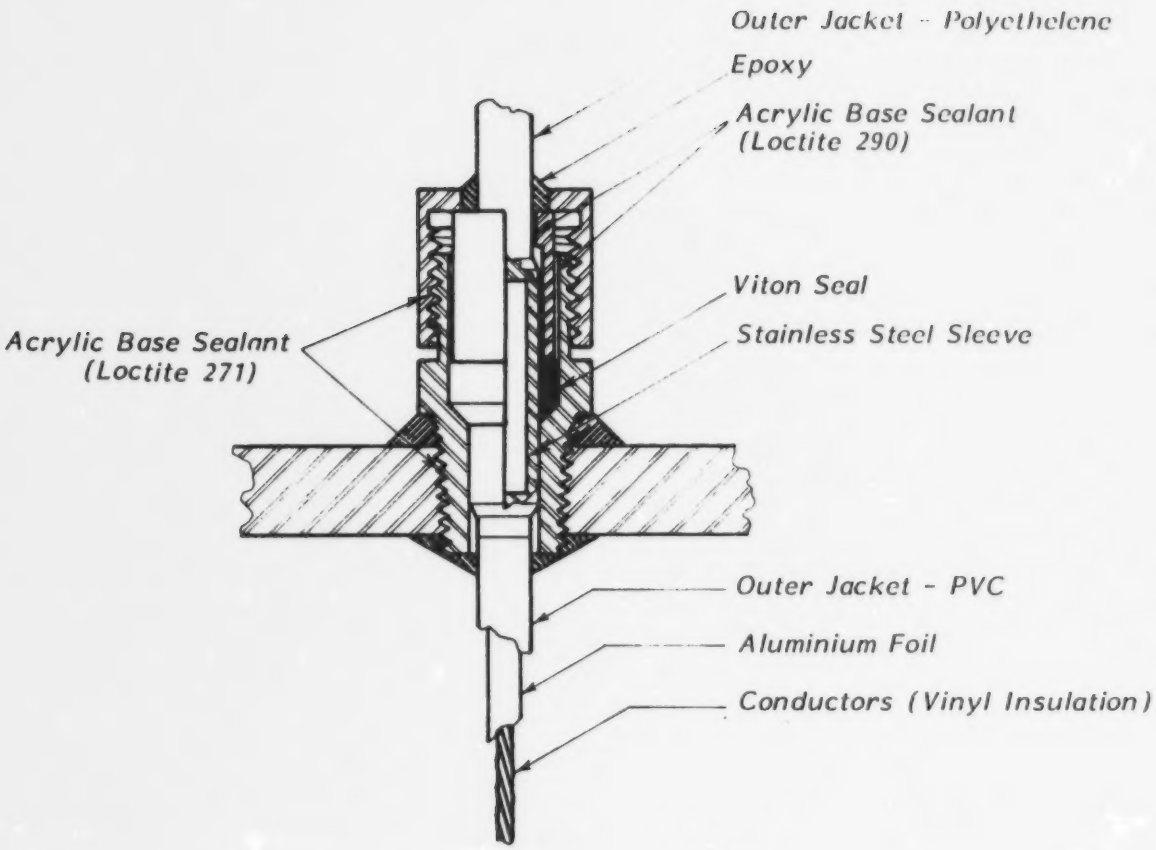

FIGURE A3-4

**CROSS SECTION OF CONAX MPG - 125 FITTING (MODIFIED)
FOR PASSAGE OF SIGNAL WIRE**

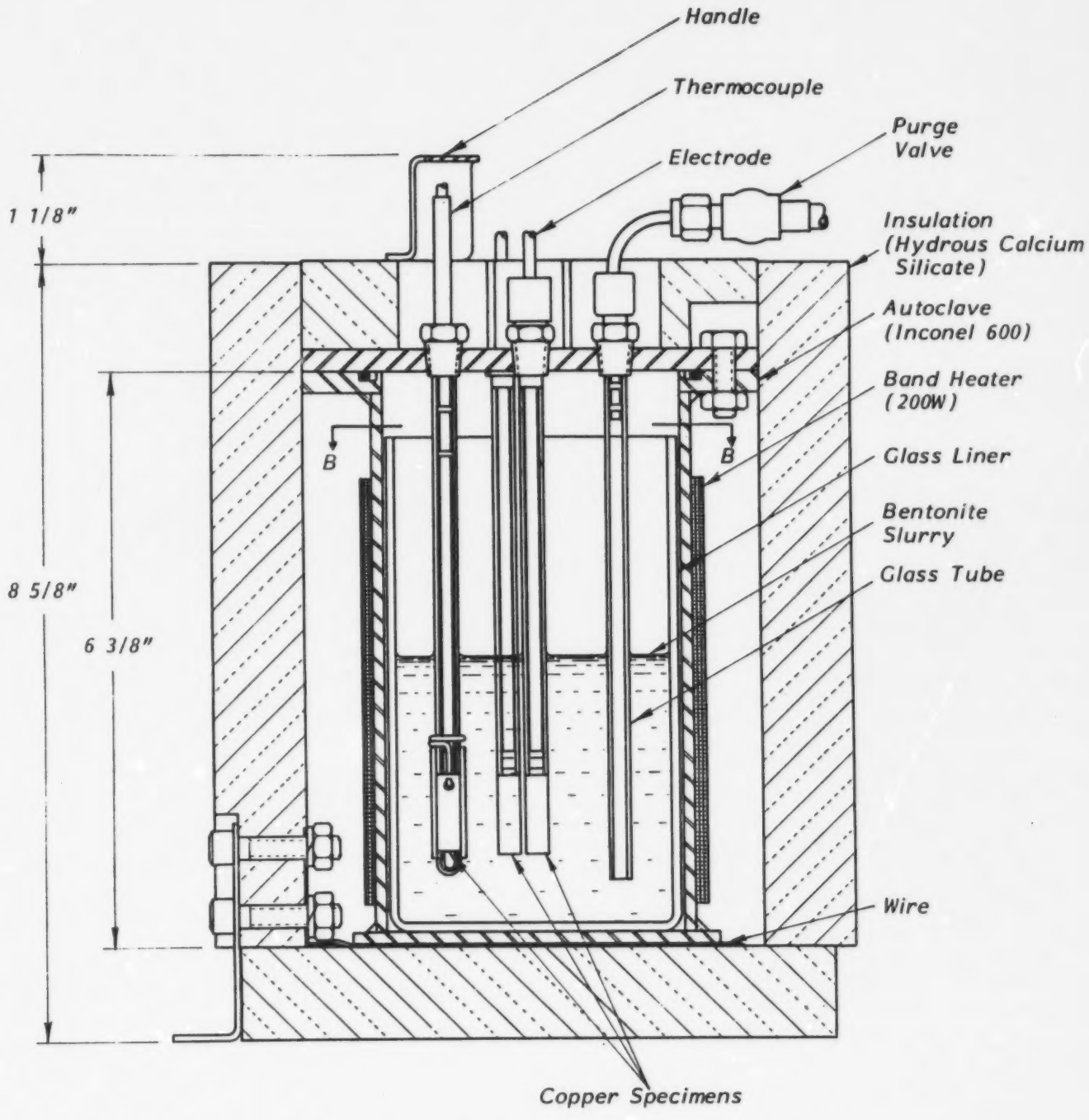

FIGURE A3-5

CROSS SECTION OF AUTOCLAVE ASSEMBLY

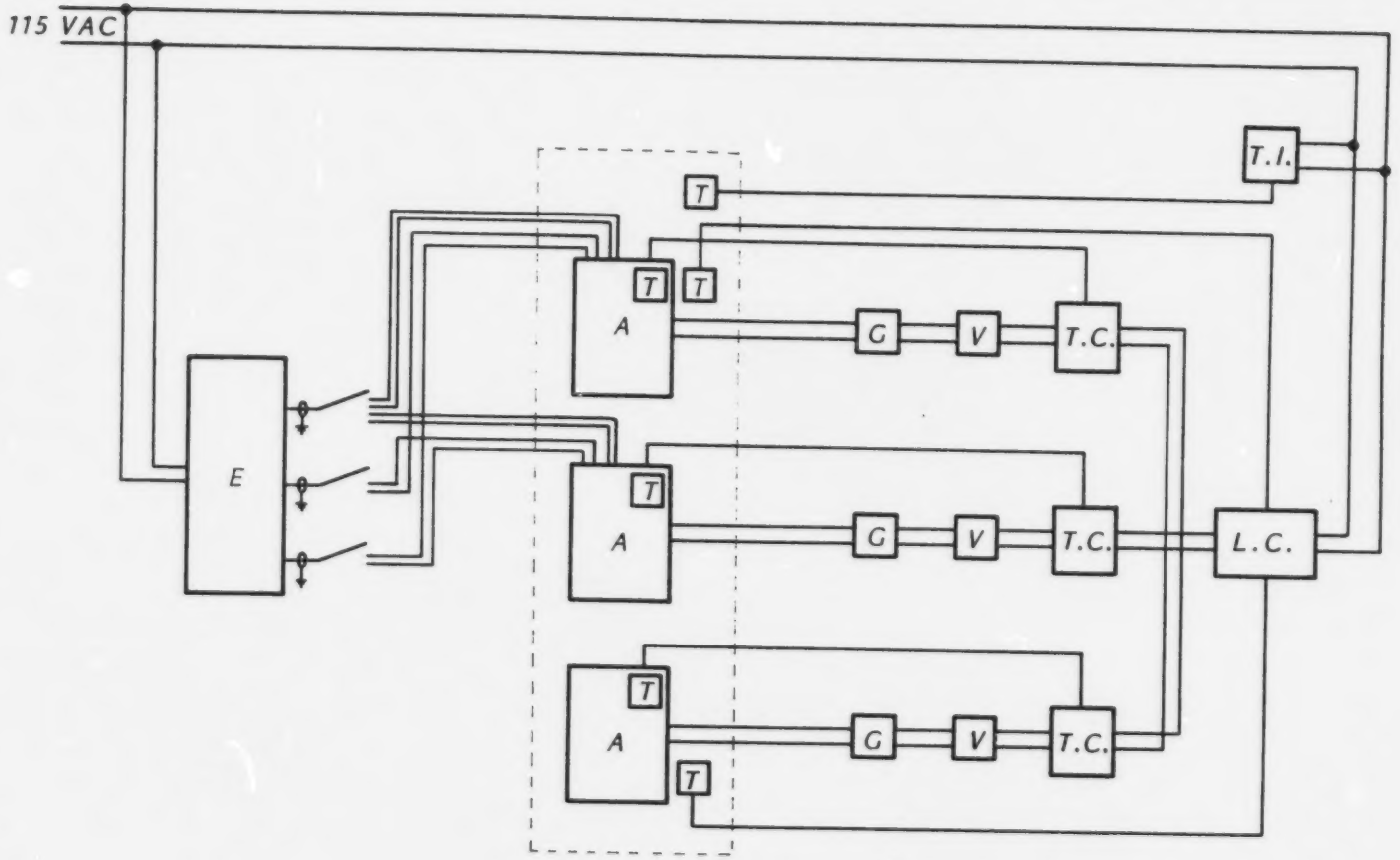

A: Autoclave (200 Watt)
E: Electrochemical Instrumentation
T: Thermocouple
T. C: Temp. Controller (and Indicator)
T. I: Temp. Indicator
G: Ground Fault Detector
V: Variable Transformer
L. C: Limit Control

FIGURE A3-6

BLOCK DIAGRAM OF ELECTRICAL CIRCUITS FOR RADIOLYSIS EXPERIMENTS

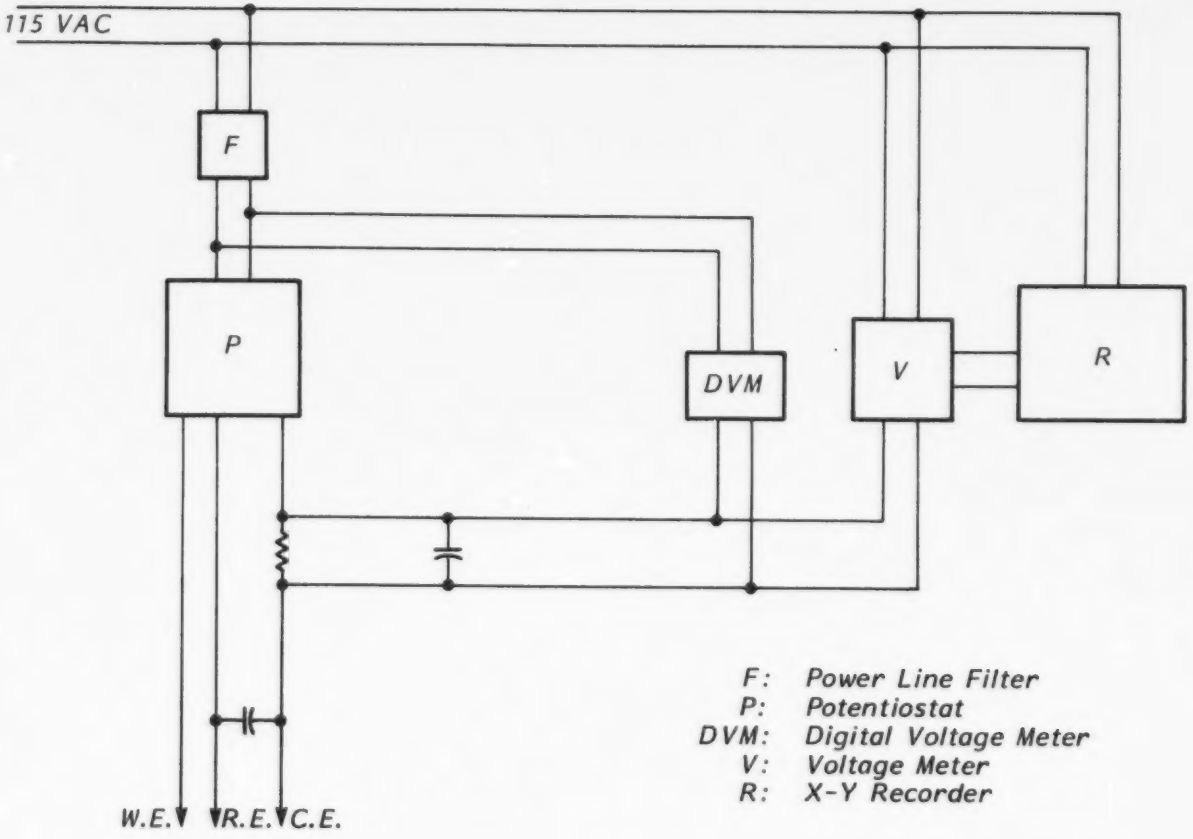

FIGURE A3-7

BLOCK DIAGRAM OF ELECTROCHEMICAL INSTRUMENTATION FOR RADIOLYSIS EXPERIMENTS